CONFIDENTIAL
SECURITY INFORMATION

NACA RM-A52I17
Copy 61
RM A52I17

NACA RM A52I17

CASE FILE COPY

UNCLASSIFIED

NACA

RESEARCH MEMORANDUM

LATERAL AND DIRECTIONAL DYNAMIC-RESPONSE CHARACTERISTICS OF A 35° SWEPT-WING AIRPLANE AS DETERMINED FROM FLIGHT MEASUREMENTS

By William C. Triplett and Stuart C. Brown

Ames Aeronautical Laboratory
Moffett Field, Calif.

GROUP 4
Downgraded at 3 year intervals; declassified after 12 years

Classification Changed to UNCLASSIFIED
Authority DOD DIR 5200.10
Date 3-16-66 By N. Devereux/

CLASSIFIED DOCUMENT
This material contains information affecting the National Defense of the United States within the meaning of the espionage laws, Title 18, U.S.C., Secs. 793 and 794, the transmission or revelation of which in any manner to an unauthorized person is prohibited by law.

NATIONAL ADVISORY COMMITTEE FOR AERONAUTICS

WASHINGTON

December 12, 1952

UNCLASSIFIED

CONFIDENTIAL

DEC 22 1952

LIBRARY
CALIFORNIA INSTITUTE OF TECHNOLOGY

This document contains information affecting the National Defense of the United States, within the meaning of the Espionage Laws, Title 18, U.S.C. Sections 793 and 794. Its transmission or the revelation of its contents in any manner to an unauthorized person is prohibited by law.

NACA RM A52I17

CONFIDENTIAL

UNCLASSIFIED

GROUP 4
Downgraded at 3 year intervals; declassified after 12 years

NATIONAL ADVISORY COMMITTEE FOR AERONAUTICS

RESEARCH MEMORANDUM

LATERAL AND DIRECTIONAL DYNAMIC-RESPONSE CHARACTERISTICS OF A 35° SWEPT-WING AIRPLANE AS DETERMINED FROM FLIGHT MEASUREMENTS

By William C. Triplett and Stuart C. Brown

SUMMARY

Lateral and directional dynamic-response characteristics of a 35° swept-wing fighter-type airplane determined from flight measurements are presented and compared with predictions based on theoretical studies and wind-tunnel data. Flights were made at altitudes of 10,000 and 35,000 feet covering the Mach number ranges of 0.50 to 0.81 and 0.50 to 1.04, respectively. Recorded data consisted of transient responses in yawing velocity, rolling velocity, and sideslip angle to pulse-type motions of the rudder and of the ailerons. These transient data were converted into frequency-response form by means of the Fourier transformation and compared with predicted responses calculated from the basic equations of motion. The equations, or transfer functions, that best describe the various measured responses were evaluated by a curve-fitting process involving the use of templates and an analogue computer. By this method it was generally possible to find equations, of simple form, that closely matched the experimental frequency responses between 1 and 10 radians per second and at the same time adequately described the recorded time histories.

Experimentally determined transfer functions were used for the evaluation of the stability derivatives that have the greatest effect on the dynamic response of the airplane. The values of these derivatives, in general, agreed favorably with predictions over the Mach number range of the test. There were notable exceptions, however, in some cases at the flight altitude of 10,000 feet. These discrepancies are attributed to aeroelastic deformations of the wing and tail.

Another departure from theory was disclosed by evaluations of the spiral root which was many times larger than expected.

UNCLASSIFIED

CONFIDENTIAL

Classification Changed to
UNCLASSIFIED
Authority
DOD DIR. 5200.10
Date 3-26-66 | By N. Devereux/

INTRODUCTION

This report describes the second phase of a flight-test program being conducted by the NACA for the purpose of determining the dynamic-response characteristics of a 35° swept-wing fighter-type airplane. The first phase of this program, which considered only the longitudinal case, was reported in reference 1. The present report applies the methods of reference 1 to the lateral- and directional-response characteristics of the test airplane. Frequency responses and the associated aerodynamic derivatives are evaluated from records taken throughout the Mach number ranges of 0.50 to 1.04 at an altitude of 35,000 feet and 0.50 to 0.81 at 10,000 feet.

The test procedures and analysis methods used are essentially the same as described in reference 1. Transient responses to both rudder and aileron disturbances are measured and analyzed to give frequency responses of yawing velocity, rolling velocity, and sideslip angle. Responses to transient rather than sinusoidal control inputs have been chosen for analysis because of convenience in making flight measurements. While certain aerodynamic information can be determined directly from transient time histories, the use of the frequency response concept allows a more complete evaluation of the dynamic behavior of the aircraft. The effects of different modes on the over-all motion can often be shown more clearly in the frequency plane, especially when these motions are complicated by structural deformation.

In this investigation, transfer functions with numerical coefficients are obtained directly from the measured frequency responses. Supplementary calculations are then made to evaluate those aerodynamic derivatives that exert the strongest influence on the airplane response. Data of this type are of particular interest in the study of airplane-autopilot combinations. Knowledge of the airplane transfer functions is necessary in the determination of the dynamic characteristics that are required of an autopilot to satisfactorily control the aircraft.

Wherever possible the results of these tests are compared with predictions based on wind-tunnel and theoretical data and also with the results of other flight tests.

NOTATION

C_L lift coefficient

C_l rolling-moment coefficient

C_n yawing-moment coefficient

C_Y side-force coefficient

D the operator $\left(\frac{d}{dt}\right)$

I_X moment of inertia about the X axis, slug-feet squared

I_Z moment of inertia about the Z axis, slug-feet squared

I_{XZ} product of inertia, slug-feet squared

R,I real and imaginary parts of a complex quantity

S wing area, square feet

V velocity, feet per second

W weight of airplane, pounds

b wing span, feet

g acceleration due to gravity, feet per second squared

i $\sqrt{-1}$

m mass of airplane, slugs

p rolling velocity, radians per second

q dynamic pressure, pounds per square foot

r yawing velocity, radians per second

t time, seconds

α angle of attack, degrees

β sideslip angle, radians (except as noted)

γ flight path angle, degrees

δ control deflection, radians (except as noted)

δ_a total aileron deflection, radians

δ_r rudder deflection, radians (except as noted)

ζ damping ratio

λ root of the characteristic equation

σ real part of a complex root

φ angle of bank, radians

Φ phase angle, degrees

ψ angle of yaw, radians

ω frequency, radians per second

ω_l natural frequency of oscillation, radians per second

ω_n undamped natural frequency, radians per second

C_{l_p} $\frac{\partial C_l}{\partial(pb/2V)}$, per radian

C_{l_r} $\frac{\partial C_l}{\partial(rb/2V)}$, per radian

C_{l_β} $\frac{\partial C_l}{\partial \beta}$, per radian

C_{n_p} $\frac{\partial C_n}{\partial(pb/2V)}$, per radian

C_{n_r} $\frac{\partial C_n}{\partial(rb/2V)}$, per radian

C_{n_β} $\frac{\partial C_n}{\partial \beta}$, per radian

C_{Y_β} $\frac{\partial C_Y}{\partial \beta}$, per radian

C_{l_δ} $\frac{\partial C_l}{\partial \delta}$, per radian

C_{n_δ} $\frac{\partial C_n}{\partial \delta}$, per radian

C_{Y_δ} $\frac{\partial C_Y}{\partial \delta}$, per radian

$C_{l_{\dot{p}}}$ $\frac{\partial C_l}{\partial \dot{p}}$, seconds squared per radian

L_p $\frac{qSb^2}{2VI_X} C_{l_p}$, per second

L_r $\frac{qSb^2}{2VI_X} C_{l_r}$, per second

L_β $\frac{qSb}{I_X} C_{l_\beta}$, per second squared

N_p $\frac{qSb^2}{2VI_Z} C_{n_p}$, per second

N_r $\frac{qSb^2}{2VI_Z} C_{n_r}$, per second

N_β $\frac{qSb}{I_Z} C_{n_\beta}$, per second squared

Y_β $\frac{qS}{mV} C_{Y_\beta}$, per second

L_δ $\frac{qSb}{I_X} C_{l_\delta}$, per second squared

N_δ $\frac{qSb}{I_Z} C_{n_\delta}$, per second squared

Y_δ $\frac{qS}{mV} C_{Y_\delta}$, per second

r_X $\frac{I_{XZ}}{I_X}$

r_Z $\frac{I_{XZ}}{I_Z}$

K_1 $\frac{g}{V} \cos \gamma$, per second

K_2 $\frac{g}{V} \sin \gamma$, per second

$L_p' \quad L_p + r_X N_p$

$L_\beta' \quad L_\beta + r_X N_\beta$

$N_r' \quad N_r + r_Z L_r$

$N_\beta' \quad N_\beta + r_Z L_\beta$

$L_\delta' \quad L_\delta + r_X N_\delta$

$N_\delta' \quad N_\delta + r_Z L_\delta$

TEST EQUIPMENT

The test airplane was a standard North American F-86A-5 with external instrument booms added as shown in figures 1 and 2. The physical characteristics of this airplane are described in table I.

Standard NACA instruments were used to record airspeed, altitude, rolling and yawing velocities, normal acceleration, angle of attack, sideslip angle, and rudder and aileron positions. All recordings were synchronized at 0.1-second intervals by a common timing circuit. The true Mach number was obtained from the nose-boom airspeed system described in reference 2.

Rate gyros were used to measure yawing and rolling velocities about the reference axes of the airplane. The yaw rate gyro had a range of ±0.5 radians per second and a natural frequency of 10 cycles per second. Corresponding values for the roll rate gyro were ±2.0 radians per second and 18 cycles per second, respectively. In both cases the damping ratios were approximately 0.7. Sideslip angles were measured by a vane-type pickup and recorded on an oscillograph. Rudder and aileron deflections were measured by control position recorders that were linked directly to the control surfaces.

The dynamic characteristics of recording instruments are of extreme importance in investigations of this type. A flight record in general contains the combined response of the airplane and recording instrument. If the instrument has a linear second-order response with known damping ratio and natural frequency, then its response can be subtracted from the combined response in the frequency plane. Obviously, it is desirable to use instruments with characteristics such that the necessary corrections are a minimum (i.e., high natural frequency and damping ratio of approximately 0.7).

The two rate gyros (rolling and yawing velocities) used in the present investigation were considered to be very satisfactory in this respect and no corrections were applied to the data. Because the response of the sideslip vane, however, was unknown and suspected to be nonlinear, results obtained from this instrument were not considered reliable at high frequencies. The control position recorders (aileron and rudder) also had unknown frequency responses but tests of similar installations have indicated very high natural frequencies, so they were assumed to give valid records over the frequency range of interest.

TEST PROCEDURE

The flight procedures consisted essentially of recording airplane responses to both aileron and rudder disturbances. Pulse-type inputs were used in all but one flight run. All flights were made at altitudes of 10,000 and 35,000 feet in the Mach number ranges of 0.50 to 0.81 and 0.50 to 1.04, respectively. The corresponding trim lift coefficients varied from 0.17 to 0.07 and 0.51 to 0.12, respectively.

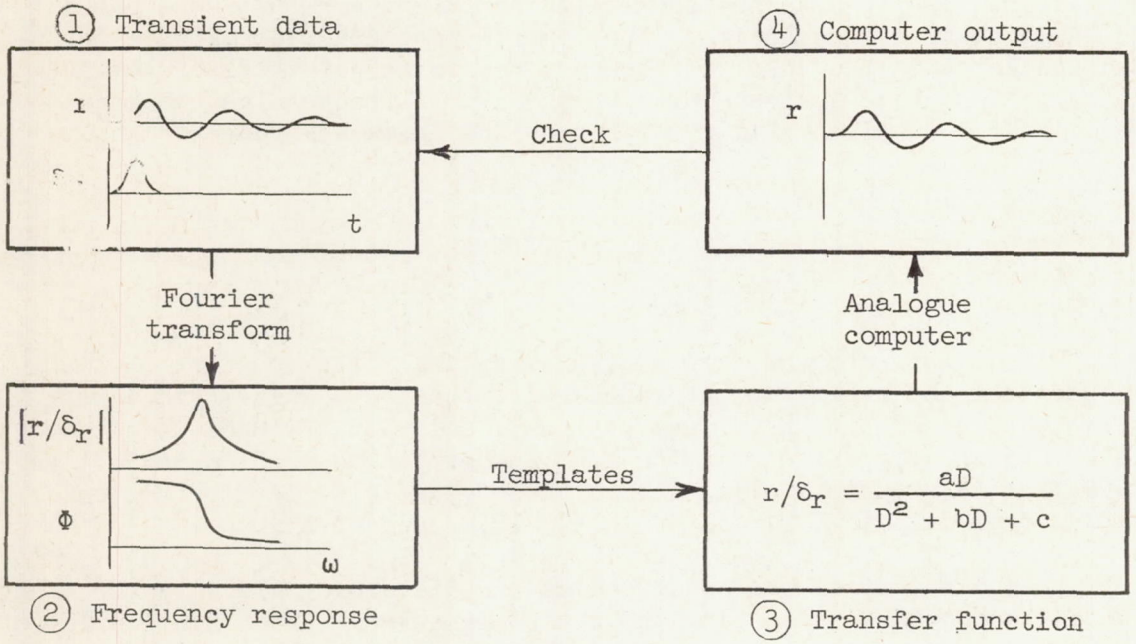
When one control was specified as the disturbing element, the other control was held fixed during the entire maneuver. After application of the pulse input, both controls were held fixed until the oscillatory motion of the aircraft had essentially subsided. The airplane responses used in the analysis were rolling velocity, yawing velocity, and sideslip angle. Sample time histories of the responses of the quantities to the appropriate control inputs can be seen in figure 3.

All flight runs at speeds below a Mach number of 0.95 were made in trimmed level flight, but to obtain data at the higher speeds it was necessary to dive the airplane. Flight altitudes changed as much as 2,000 feet during each diving run although there was little variation in Mach number. For analysis purposes the altitude and dynamic pressure were assumed to be constant at their average values during each run.

METHOD OF ANALYZING EXPERIMENTAL DATA

The basic method used in the analysis of the transient flight data was described fully in reference 1 but is briefly summarized here.

The evaluation of the transfer functions that describe the motions of the airplane were carried out as indicated in the sketch:



The transient responses were first corrected wherever necessary so that the measurements would conform to the stability axes notation that is commonly used. This correction is explained in appendix A. The data were then analyzed to obtain the Fourier transformations by means of an IBM machine calculating method employing an adaption of Simpson's rule. These calculations were carried out at a number of frequencies between 0.5 and 16 radians per second. The resultant frequency responses were plotted as shown in the form of amplitude ratios and phase angles.

As discussed in appendix B, the type of input used in flight definitely places a limit on the accuracy of the Fourier analysis of a transient record. In general, to obtain the widest usable frequency range a pulse-type input should be used. When low frequencies (below 1 radian per second) are desired, a step input is preferable although this type of disturbance may result in motions that exceed the ranges of linearity. The method used, while subject to these limitations, is extremely accurate provided that the flight records are tabulated at enough time intervals to clearly define the data.

The second step consisted of fitting the graphical frequency responses to a set of dynamic response templates which define the first- and second-order complex functions $1 + iu$ and $1 + 2\zeta iu - u^2$ where u is

a nondimensional frequency variable and ζ the damping ratio. This set of templates, as described in reference 3, contained one pair of first-order curves (amplitude and phase) and a family of second-order curves with different values of the parameter ζ. By combining templates in the proper manner it was generally possible to find one combination that would closely match both amplitude ratio and phase-angle plots. This particular combination defines the equation, with approximate numerical coefficients, that most nearly describes the graphical frequency response. This equation is normally referred to as the transfer function.

The final step of the analysis involves the use of an analogue computer on which the airplane transfer functions are set up. If a time history of an actual recorded control motion is supplied as an input to the computer, then the output should be indentical to the response measured in flight. Since the templates give only approximate values of the coefficients, these values were altered until the output of the computer satisfactorily matched the experimental time response. Thus, in addition to refining the results, the computer automatically furnishes a check on the previous computations.

After the transfer functions that describe the various airplane responses were obtained, the stability derivatives C_{n_β}, C_{l_β}, C_{n_r}, C_{l_p}, $C_{l_{\delta_a}}$, and $C_{n_{\delta_r}}$ were evaluated as explained in a later section.

RESULTS AND DISCUSSION

The results discussed in the following paragraphs were obtained from transient time histories as explained in the previous section. Flight evaluated frequency responses, transfer functions, and stability derivatives are presented and compared with predictions based on wind-tunnel data and theoretical studies.

Frequency Responses

Plotted in figure 4 are typical flight evaluated frequency responses of rolling velocity, yawing velocity, and sideslip angle to rudder and also to aileron inputs. These were all obtained at an altitude of 35,000 feet; responses for 10,000 feet showed similar characteristics and have not been plotted. The purpose of these figures is to show general trends with varying Mach number, and therefore smooth curves have been faired through the calculated test points. In most cases more than one flight record was analyzed at each flight speed in order to check the data for consistency. Only at the highest test speeds (above a Mach number of 1.0) was there appreciable inconsistency.

The responses to rudder inputs have not been plotted at frequencies greater than 8 radians per second because there was considerable scatter and also a lack of well-defined trends in the data at the higher frequencies. The aileron responses, however, are shown to 16 radians per second. Wherever necessary for clarity or because of erratic data, parts of some of the curves have been omitted. The β/δ_a response is shown at only three speeds because of a failure in the sideslip-angle recording system.

With minor exceptions, the curves show consistent and gradual variations with Mach number. One such exception can be seen in figures 4(d) and 4(e) where the amplitudes of p/δ_a and r/δ_a at a Mach number of 0.61 lack the customary resonant peaks. This is the result of time histories in which there was no oscillatory motion. This unusual characteristic can be explained by reference to the predicted transfer functions developed in appendix C and discussed in the following section. The predicted p/δ_a response equation for a Mach number of 0.6 at 35,000 feet is

$$\frac{p}{\delta_a} = \frac{21.1(D^2+0.455D+6.74)}{(D+0.00113)\ (D+2.203)\ (D^2+0.438D+7.25)}$$

It can be seen that the two quadratic terms are nearly identical and thus the oscillatory mode is effectively canceled. Since rolling and yawing motions are coupled, the r/δ_a response must exhibit the same characteristics at this particular speed.

Another interesting point with regard to figure 4(e) is the wide variation in phase angles at different flight speeds. Predicted transfer functions indicate that at low speeds (below a Mach number of 0.7) where $C_{n_{\delta_a}}$ is negative, the phase angles approach -270° asymptotically with increasing frequency. Unpublished wind-tunnel data indicate that near a Mach number of 0.7 there is a transition in which $C_{n_{\delta_a}}$ becomes positive and consequently three of the coefficients in the numerator of the transfer function change sign. The result is an increase of 180° in the high frequency phase lag.

The frequency-response test points derived from flight data at a Mach number of 0.81 have been replotted in figure 5 which shows all six responses for the 35,000 foot altitude and the r/δ_r and p/δ_a responses for 10,000 feet. These results are typical in indicating the degree of scatter usually encountered in the Fourier analysis of a particular flight record. Plotted as solid lines for comparison are predicted responses that have been calculated using estimates of the various stability derivatives presented in table II, which were obtained from reference 4 and also from wind-tunnel tests by the manufacturer. These calculations were made as shown in appendix C, using the exact linear fourth-order response equations. The agreement between measured and

predicted responses is generally good except, in some cases, at the extremes of the test frequency range.

In addition to the pulse-type inputs, a step disturbance of the rudder was used in one instance at a Mach number of 0.81 in order to more clearly define the low frequency portions of the p/δ_r and r/δ_r frequency responses. Results of this analysis from 0.1 to 1.0 radians per second are plotted in figures 5(a) and 5(b) and are discussed in more detail in a later section.

Also shown as dotted lines in figures 5(b), 5(c), 5(d), 5(g), and 5(h) are responses computed from predicted transfer functions that have been simplified as indicated in the following paragraphs.

Theoretical Transfer Functions

It is shown in appendix C that the characteristic equation Δ can be factored into the form

$$\Delta = D(D-\lambda_1)\ (D-\lambda_2)\ (D^2+c_1D+c_2)$$

where λ_1 and λ_2 are the spiral and rolling roots, respectively, and where c_1 and c_2 are coefficients that define the oscillatory mode. By neglecting λ_1 (which is usually very small) and by omitting other small terms that appear in the numerators of the various response equations, three of the six responses may be reduced to the following simple forms:

$$\left.\begin{aligned} \frac{r}{\delta_r} &= \frac{B_3D}{D^2+c_1D+c_2} \\ \frac{\beta}{\delta_r} &= \frac{-B_3}{D^2+c_1D+c_2} \\ \frac{p}{\delta_a} &= \frac{A_3}{D-\lambda_2} \end{aligned}\right\} \qquad (1)$$

It is also shown that by making additional assumptions as to relative magnitudes, the coefficients λ_2, c_1, and c_2 can be expressed as L_p, $-(N_r+Y_\beta)$, and N_β', respectively. Furthermore, since $B_3 \equiv N_{\delta_r}'$ and $A_3 \equiv L_{\delta_a}'$, equations (1) can be written as

$$\frac{r}{\delta_r} = \frac{N_{\delta_r}'D}{D^2-(N_r+Y_\beta)D+N_\beta'} \qquad (2a)$$

$$\frac{\beta}{\delta_r} = \frac{-N_{\delta_r}}{D^2-(N_r+Y_\beta)D+N_\beta'} \tag{2b}$$

$$\frac{p}{\delta_a} = \frac{L_{\delta_a}'}{D-L_p} \tag{2c}$$

It can be seen that in equations 2(a) and 2(b) the spiral and rolling modes are completely neglected, and yet, as shown in figures 5(b), 5(c), and 5(g), these simplified transfer functions yield responses that are almost identical to those obtained from the "exact" equations for frequencies greater than 1 radian per second. Similarly, the response computed from equation 2(c) closely matches the exact response (fig. 5(d)) over the frequency range shown except that it omits the small peak normally associated with the oscillatory mode. The spiral mode which has been neglected in all three simple equations appears to have no effect on the calculated airplane response except at frequencies well below 0.1 radian per second.

Experimentally Determined Transfer Functions

In the analysis of the flight data it was found that the frequency responses of r/δ_r, β/δ_r, and p/δ_a could be successfully simulated by simple transfer functions of the same forms as equations (1). Solutions of these equations on the analogue computer, using final "best" values of the numerical coefficients with actual control motions as recorded in flight, resulted in outputs that closely matched the measured time histories of r, β, and p as shown in figure 3. This fact implies that the modes of motion that are neglected in each case have very little effect on the time response to a pulse-type input.

By use of the coefficients that best describe the measured time histories, frequency responses were calculated for comparison with those derived directly from flight data. Examples of these calculations are shown by the dash-dot lines in figures 5(b), 5(d), 5(g), and 5(h). These curves, in general, match the experimental points closely for frequencies between 1 and 10 radians per second.

The experimentally determined values of the coefficients λ_2, c_1, and c_2 (using the notation of equations (1)) have been plotted in figure 6 and are compared to predicted values of the same coefficients that were obtained by factoring predicted characteristic equations for several different Mach numbers. To give some idea of the errors involved in the assumptions of equations (2), predicted values of L_p, $N_r + Y_\beta$, and N_β'

have also been plotted for comparison with the coefficients λ_2, c_1, and c_2. It appears that, for this particular airplane, the assumptions are valid and that the simplified transfer functions form a logical basis for the evaluation of stability derivatives. The flight evaluated coefficients c_1 and c_2 have been transformed into the customary undamped natural frequency and damping ratio designations and are plotted in this form in figure 7.

It is apparent from equations 2(a) and 2(b) that the same information can be obtained from either r/δ_r or β/δ_r. Coefficients evaluated from each of these responses agreed favorably in most cases; however, because of indications that the yaw rate gyro possessed dynamic characteristics superior to those of the sideslip vane, only the yawing velocity responses were used in the final calculations.

The transfer functions of the three remaining responses p/δ_r, r/δ_a, and β/δ_a were not amenable to simplification. However, it was found that the p/δ_r response could be matched satisfactorily by a transfer function of the type

$$\frac{p}{\delta_r} = \frac{a_1(D+a_2)\ (D+a_3)}{(D-\lambda_2)\ (D^2+c_1D+c_2)}$$

which is the same form as developed in appendix C except that the spiral mode has been neglected. As written here, a_1 is identical to L_{δ_r}' while a_2 and a_3 are complicated combinations of derivatives that cannot be readily simplified. Although this equation closely describes the measured time histories (fig. 3), it was difficult to find unique values of the numerator coefficients. Changes in one of these could be compensated for by corresponding changes in the other two, and the values were not considered to be reliable enough for presentation.

Definition of the r/δ_a and β/δ_a responses required fourth-order transfer functions that include all three modes, and because of practical difficulties involved no attempt was made to evaluate the coefficients of these responses.

Stability Derivatives

In addition to the quantities L_p, $N_r + Y_\beta$, N_β', N_{δ_r}', and L_{δ_a}', that were determined as mentioned in the preceding paragraphs, the coefficient L_β' was evaluated from the time histories of rolling and yawing velocity as shown in reference 5. This method is briefly outlined in appendix D.

The quantities N_β, L_β, N_{δ_r}, and L_{δ_a} can then be calculated from N_β', L_β', N_{δ_r}', and L_{δ_a}' by using the following expressions obtained from the relationships developed in appendix C:

$$N_\beta = \frac{N_\beta' - r_Z L_\beta'}{1 - r_X r_Z}$$

$$L_\beta = \frac{L_\beta' - r_X N_\beta'}{1 - r_X r_Z}$$

$$N_{\delta_r} = \frac{N_{\delta_r}' - r_Z L_{\delta_r}'}{1 - r_X r_Z}$$

$$L_{\delta_a} = \frac{L_{\delta_a}' - r_X N_{\delta_a}'}{1 - r_X r_Z}$$

Because r_X and r_Z are very small quantities, wind-tunnel estimates of L_{δ_r}' were assumed to be sufficiently accurate to use in the calculation of N_{δ_r}. The term $r_X N_{\delta_a}'$ was completely neglected in evaluating L_{δ_a}.

Finally, from the definitions given in the notation it is possible to evaluate the derivatives C_{l_p}, C_{n_β}, C_{l_β}, $C_{n_{\delta_r}}$, and $C_{l_{\delta_a}}$.

The analysis methods used herein do not allow the separation of the damping term $N_r + Y_\beta$. As compared to N_r, the term Y_β is small and can generally be predicted accurately from wind-tunnel measurements. Therefore values of C_{Y_β} given in table II were used in calculating C_{n_r} from the quantity $N_r + Y_\beta$.

The flight evaluated derivatives for both altitudes are plotted against Mach number in figures 8 and 9. These are compared to the predicted values listed in table II. Through the speed range of the test the predictions for both altitudes are essentially the same, except as noted in the plot of C_{l_β}.

The correlation between predicted derivatives and those evaluated from flight at 35,000 feet is generally good except, in some cases, at speeds near a Mach number of 1.0 where the predictions are apt to be inaccurate. Unpredicted variations with altitude are also apparent in the flight values of C_{l_p}, C_{n_r}, and $C_{n_{\delta_r}}$. At a Mach number of 0.8 the

value of C_{n_r} for 10,000 feet is less than one half the value at 35,000 feet. Flight data of reference 4 when expressed in this form show a similar trend. The plot of $C_{n_{\delta_r}}$ indicates the same tendency to a lesser degree, while the 10,000-foot value of C_{l_p} (at M = 0.8) is some 50 percent higher than the value at 35,000 feet.

Values of C_{l_β} determined in the present investigation agree favorably with wind-tunnel results, while those reported in reference 6 (obtained from static flight tests of the same airplane) are much smaller in magnitude. It appears, however, that the results of reference 6 are subject to error because of the simplifying assumptions made. A more rigorous approach would have resulted in larger values of this derivative.

Examination of figure 9 shows the control effectiveness derivatives $C_{n_{\delta_r}}$ and $C_{l_{\delta_a}}$ to have similar variations with increasing Mach number, and in each case the measured values are generally smaller than predicted. Values of $C_{l_{\delta_a}}$ obtained in the present investigation agree closely with those presented in reference 7 which again were evaluated from flight measurements of the same airplane.

In this investigation there was no evidence of nonlinear variations of rolling or yawing-moment coefficients with p, r, or β. This was concluded because (1) the period and damping of the oscillations following a control input were essentially constant in every case (no systematic variations with amplitude), and (2) the experimental time histories could be matched, in general, by differential equations with constant coefficients.

No conclusions are drawn as to nonlinear moment coefficient variations with δ_a or δ_r because the magnitudes of the control inputs were not varied appreciably during the tests. They were small enough, however, so that it could be assumed that the linear ranges were not exceeded.

Aeroelastic Effects

Although the present investigation was not conducted for the purpose of studying aeroelasticity, the test results do show the influence of structural deformation as indicated in the discussion that follows.

Effects at high frequency.- The frequency-response measurements of p/δ_a indicate a mode of motion at high frequencies that is not consistent with the rigid-airplane equations given in appendix C. According to these equations, the amplitude of this response should approach zero (at a slope of -1 on a logarithmic plot) as frequency increases, while the phase angle approaches -90° asymptotically. Examination of

figure 5(d), however, shows an increase in phase angle and a gradual decrease in amplitude attenuation at frequencies greater than 10 radians per second. These data indicate the presence of an additional high frequency mode which conceivably could correspond to the primary bending frequency of the airplane wing (about 8 cps). A mode of this type can be included in the equations of motion, in general, by introducing additional degrees of freedom which will relate the mass and stiffness characteristics of the wing to actual motions of the airplane. From purely geometric considerations, bending of a swept-back wing is accompanied by a change in angle of attack and, when the motions of the two wing panels are out of phase, there is a resultant rolling moment. Thus it is reasonable to expect wing bending or twist to have a noticeable effect on the rolling response of the airplane.

Effects on flight evaluated stability derivatives.- Test values of C_{l_p} shown in figure 8 indicate a variation not only with Mach number but also with altitude (dynamic pressure) which may be the result of inertia loading.

When the airplane is accelerated in roll, inertia forces cause the two wing panels to bend in opposite directions. The resulting angle-of-attack variation produces a moment that tends to modify the rate of roll. This effect can be considered in the basic equations of motion by the introduction of $\partial C_l/\partial \dot{p}$, the variation of rolling-moment coefficient with rolling acceleration. Then letting

$$L_{\dot{p}} = \frac{qSb}{I_X} \frac{\partial C_l}{\partial \dot{p}}$$

equation (C4) may be written as

$$\left[(1-L_{\dot{p}})D^2 - L_p D\right]\varphi + (-r_X D^2 - L_r D)\psi - L_\beta \beta = L_{\delta_a} \delta_a$$

It should be noted that the inclusion of $L_{\dot{p}}$ is analogous to a change in the moment of inertia about the X axis.

If each term is divided by $(1 - L_{\dot{p}})$ then this equation is parallel in form to equation (C4), and the simplified transfer function for p/δ_a becomes

$$\frac{p}{\delta_a} = \frac{L_{\delta_a} / 1-L_{\dot{p}}}{D-(L_p/1-L_{\dot{p}})}$$

Thus it appears that the two derivatives as evaluated from flight data are actually $C_{l_p}/(1 - L_{\dot{p}})$ and $C_{l_{\delta_a}}/(1 - L_{\dot{p}})$. For a swept-back wing $L_{\dot{p}}$ is a positive quantity that increases with dynamic pressure; so the

measured values of the two derivatives should also increase with dynamic pressure.

The test measurements of C_{l_p} clearly show this trend, but in the case of $C_{l_{\delta_a}}$ there was no appreciable variation with altitude. Theoretical studies, however, and also wind-tunnel tests of flexible models (such as described in reference 8) have clearly indicated that, in the absence of inertia loads, the aileron effectiveness will in general decrease with increasing dynamic pressure, the primary contributing factor being the torsional flexibility of the wing.

It has been shown in reference 8 that the derivative C_{l_p} will also vary with dynamic pressure. For straight wings there will generally be an increase in the negative value of C_{l_p}, while for highly swept-back wings there will be a decrease. Presumably there is an intermediate sweep angle at which there is essentially no variation in C_{l_p} with dynamic pressure.

In order to substantiate this hypothesis regarding the effects of elasticity, numerical calculations were made using the method of reference 9 to estimate the variations with dynamic pressure of the quantities C_{l_p}, $C_{l_{\delta_a}}$, and $L_{\dot{p}}$. These calculations were based on information supplied by the manufacturer regarding the mass distribution and stiffness of the airplane wing. While not agreeing quantitatively with the measured variations, the results did show the same trends with dynamic pressure that were observed in the flight evaluated derivatives. More specifically, the calculations indicated that $C_{l_{\delta_a}}$ decreases much more rapidly with increasing dynamic pressure than does C_{l_p}. Furthermore, the variation of $(1 - L_{\dot{p}})$ was approximately the same as that of $C_{l_{\delta_a}}$. This indicates that an increase in the effective derivative $C_{l_p}/(1 - L_{\dot{p}})$ with dynamic pressure can be expected even though there is little variation in $C_{l_{\delta_a}}/(1 - L_{\dot{p}})$.

Similar arguments may be advanced to explain the altitude variations that were noted in C_{n_r} and $C_{n_{\delta_r}}$. These variations could be the result of distortions of the fuselage and tail due to inertia and aerodynamic loadings.

Response at Low Frequency

As mentioned in an earlier section, responses to a rudder step disturbance were recorded in flight in order to check mainly the low frequency portion of the r/δ_r frequency response (0 to 1.0 radians per second). As shown in figure 5(b), the results of this analysis verify

the prediction of a sharp attenuation in amplitude at a frequency of 0.4 radians per second. A step input was used in this particular case because it gives much more accurate results at low frequencies than a pulse input. The question of control inputs is discussed more fully in appendix B.

Although not shown in figure 5(b), the zero frequency (steady-state) amplitude of r/δ_r was measured to be 1.44 as contrasted to a value of 169.0 predicted from the exact equation. Similarly, the steady-state amplitude of p/δ_r was measured as 1.75, while the theoretical equations indicate that this value should be zero. These discrepancies can be partially explained in view of the following discussion.

The linear equations of motion used herein are valid only for small angular displacements. When the step disturbance was applied in flight, an angle of bank of approximately 70° was reached before the motions of the airplane became steady. In the side force equation (equation (C6)) the term $K_1\varphi$ is actually a linear approximation of $K_1 \sin \varphi$ and obviously is valid only for small bank angles. To determine the effect of this nonlinearity on the predicted airplane responses, time histories of p, r, and φ were calculated on an analogue computer for a rudder step input of the same magnitude as applied in flight. Predicted values of the various stability derivatives were used and solutions were obtained first with the linear approximation $K_1\varphi$ and next with the nonlinear $K_1 \sin \varphi$. Results obtained from the nonlinear equation indicated that the rolling velocity response would reach a finite steady-state magnitude as seen in the flight record. In the case of the yawing velocity response, however, the effect of the nonlinearity was such as to reduce the steady-state value somewhat but not nearly enough to account for the extreme difference between flight measurements and predictions.

The relationship of spiral damping to the zero frequency amplitude offers another possible explanation for this discrepancy. Although the basic analysis methods used in this report give no information concerning the spiral mode, predictions indicated that at a Mach number of 0.8 at 35,000 feet the spiral root was -0.00070 which leads to the previously mentioned steady-state magnitude of 169.0 for r/δ_r. The subsidence of this mode was clearly measurable, however, in the yawing velocity response to the rudder step input. A line was drawn through the center of the free oscillations to represent the spiral mode and the root was measured as -0.07 instead of -0.00070 as predicted.

This measurement was verified by examining recorded time histories of yawing velocity responses to aileron pulse inputs (e.g., fig. 3(b)). On eight flight records taken at Mach numbers between 0.5 and 0.9 the spiral root was found to vary from -0.06 to -0.09. It can be seen that the discrepancy in spiral subsidence is of the same order of magnitude as the discrepancy in steady-state magnitudes of r/δ_r.

In the characteristic equation the coefficient C_0 is generally very small as compared to C_1, and thus the theoretical spiral root can be expressed quite accurately as simply

$$\lambda_1 = -\frac{C_0}{C_1} \tag{3}$$

which is approximately the same as

$$\lambda_1 = \frac{K_1(L_rN_\beta - N_rL_\beta)}{-L_pN_\beta} \tag{4}$$

All the quantities on the right side of this expression except L_r have been determined experimentally and found to agree reasonably well with predicted values. Even though the term $L_rN_\beta - N_rL_\beta$ represents a small difference of two large numbers, it is inconceivable that the errors in N_β, N_r, or L_β can be of sufficient magnitude to account for the large deviation in the spiral root. Therefore it appears that this discrepancy must be at least partially due to an erroneous estimate of L_r. By rearranging terms in equation (4)

$$L_r = -\frac{\lambda_1 L_p}{K_1} + \frac{N_rL_\beta}{N_\beta}$$

Using experimental values of all quantities on the right-hand side for the case of 0.8 Mach number at 35,000 feet results in a value of -4.2 for L_r as contrasted to the original prediction of 0.844. Further study showed that the resulting value of L_r was not appreciably changed by using more exact expressions in place of equations (3) and (4). Then assuming that all experimentally determined values on the right-hand side of equation (5) are correct, C_{l_r} must have a value of -0.537 rather than 0.108 as predicted.

Effects of Minor Derivatives, Product of Inertia, and Flight-Path Angle

The results of this report indicate that a knowledge of C_{n_β}, C_{l_β}, C_{n_r}, and C_{Y_β} is sufficient to define the oscillatory mode, that the rolling mode is primarily a function of C_{l_p}, and that the spiral mode is defined by C_{l_r}, C_{n_β}, C_{n_r}, C_{l_β}, and C_{l_p}. Therefore it would appear that C_{n_p} has little effect on the dynamic behavior of the test airplane and that C_{l_r} influences only the spiral mode. Because derivatives such as C_{n_p} and C_{l_r} are usually difficult to estimate, the

question may arise as to whether large changes in either of these derivatives will appreciably alter the airplane stability. If erroneous estimates of C_{n_p} and C_{l_r} had been used in this report, would the simplifications made in appendix C still be valid? Similar questions may arise regarding the effects of product of inertia and flight-path angle. For this reason table III has been prepared. This table shows the manner in which radical changes in each of the above-mentioned quantities will effect the roots of the characteristic equation. In this example, theoretical data for a Mach number of 0.5 and an altitude of 35,000 feet were used. Sample calculations have shown that at this speed and altitude the effects to be considered are more extreme than for any of the other flight conditions covered in this investigation.

Examination of table III shows trends that have been verified in many other investigations of this type. Extremely large changes in C_{n_p} result in variations of all four of the roots although only the oscillatory damping is greatly affected. On the other hand changes in C_{l_r}, as previously intimated, cause large variations in only the spiral damping. Variations in I_{XZ} appear to influence all the roots except the spiral root, with the largest effect on the oscillatory damping. Finally the introduction of a flight-path angle into the equations changes the spiral root radically, but even for an angle of -90° there is very little effect on the other roots.

Looking at table III from a different point of view, it can be seen that the oscillatory damping is influenced to some extent by each quantity considered and thus is often difficult to predict accurately. This obviously means that the expression $N_r + Y_\beta$ may not always be adequate in defining the oscillatory damping.

CONCLUDING REMARKS

A flight investigation has been performed on a 35° swept-wing fighter-type airplane in which dynamic lateral- and directional-response characteristics were measured. Transient-type responses to rudder and aileron disturbances were recorded at altitudes of 10,000 and 35,000 feet in the Mach number ranges of 0.50 to 0.81 and 0.50 to 1.04, respectively. From the results of the analysis of these data, the following statements can be made.

Airplane responses in yawing velocity and side-slip angle due to rudder disturbances can be represented by second-order transfer functions that are related solely to the oscillatory mode. Simple first-order equations adequately define the rolling velocity response to an aileron input. It was found that these equations would closely define an entire measured time history and also describe the corresponding frequency response through the range of 1 to 10 radians per second.

Fourth-order transfer functions calculated from the basic equations of motion using wind-tunnel and theoretical estimates of the various stability derivatives can be simplified by neglecting small quantities and by making approximate cancellations until they are of the same form as those evaluated from flight data. Furthermore, it was possible to express the coefficients of these transfer functions in terms of individual stability derivatives. Frequency responses computed from these simplified equations were almost identical (between 1 and 10 radians per second) to those computed from the exact fourth-order transfer functions, and when compared with experimental results there was generally good agreement. Thus it is concluded that the simplified transfer functions form a reliable basis not only for estimating airplane responses but also for the flight evaluation of stability derivatives. The methods used here are felt to be sufficiently general to apply to any conventional airplane, with some reservation regarding the accuracy of the evaluation of C_{n_r}.

Experimental values of the derivatives C_{n_β}, C_{l_β}, C_{l_p}, C_{n_r}, $C_{n_{\delta_r}}$, and $C_{l_{\delta_a}}$ compared favorably with predictions, based on theory and wind-tunnel measurements, at Mach numbers below 0.95, while at higher speeds, where predictions are questionable, there was some deviation. There were also notable discrepancies in flight values of C_{l_p} and C_{n_r}, obtained at the 10,000 foot altitude, which were attributed to structural deformations resulting from aerodynamic and inertia loads.

When the Fourier analysis for p/δ_a was extended to frequencies beyond 10 radians per second, the frequency response showed evidence of aeroelastic deformation which appeared as an additional mode of motion not consistent with rigid airplane theory.

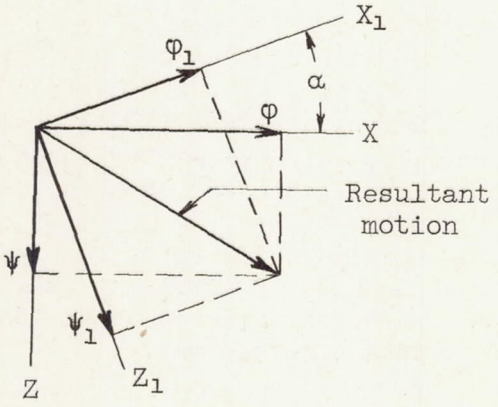
As the frequency approaches zero the spiral mode becomes the predominant factor in the airplane response. The spiral root was measured as -0.07 (at a Mach number of 0.8) which is many times greater than predicted. To satisfactorily account for this large discrepancy would require a negative value for C_{l_r} which is contrary to theoretical estimates.

Ames Aeronautical Laboratory
National Advisory Committee for Aeronautics
Moffett Field, California

APPENDIX A

TRANSFER OF AXES

The equations of motion normally used in airplane dynamics are based on a system of axes fixed in the airplane in which the X axis is the intersection of the plane of symmetry and a plane perpendicular to the plane of symmetry that contains the relative wind vector. These are normally referred to as stability or flight-path axes. The angular displacement between the X axis and the reference axis of the airplane is equal to the angle of attack. Since recording instruments are generally alined with the reference axis, measurements of angular displacements and rates must be corrected to conform to stability axes notation as indicated in the following sketch taken from reference 5. Here φ and ψ are vector components of the resultant rotation of the airplane and the subscript 1 refers to the reference or body axes.



From the sketch it can be seen that

$$\varphi = \varphi_1 \cos \alpha + \psi_1 \sin \alpha$$

$$\psi = \psi_1 \cos \alpha - \varphi_1 \sin \alpha$$

Sideslip angles can be transformed by the relation

$$\beta = \beta_1 \cos \alpha$$

For most purposes these conversions need be made only when the angle of attack is large. In this investigation it was found that the corrections to rolling velocity responses could be neglected in all cases because, for either type of input, the response in yaw is small compared to that in roll. In the case of the yawing velocity records, however,

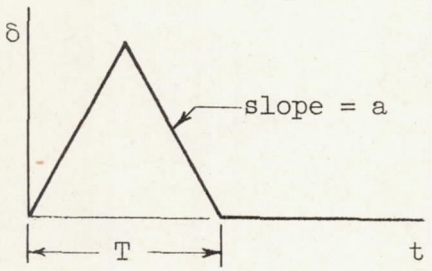
corrections were necessary. When a rudder input was used this correction was negligible at those speeds where angles of attack were less than 2°, but in the case of the yawing responses to aileron inputs the conversion had to be made at all speeds. The correction to β was neglected in every case.

APPENDIX B

CONTROL INPUTS

When frequency responses are to be calculated from transient records, care should be given to the choice of a suitable forcing function. The frequency range through which accurate transformations can be obtained is definitely limited by the shape of the control input. Theoretically, a pure impulse (zero time duration) is the most desirable input for all purposes because it gives uniform excitation to the entire frequency spectrum. The transform of a step input, on the other hand, has a magnitude that varies inversely with frequency and thus gives infinite excitation to the zero frequency component at the expense of the higher frequencies.

The nearest physical approach to a pure impulse is an input that is roughly triangular in shape as shown in the sketch:



Letting a equal the slope and T equal the time base of the triangle, the Fourier transformation of this input can be obtained from the relation

$$\delta(i\omega) = \int_0^T \delta(t) e^{-i\omega t} dt$$

Integration results in a transformation with the following real and imaginary parts:

$$R = \frac{2a}{\omega^2} \cos \frac{\omega T}{2} \left(1 - \cos \frac{\omega T}{2} \right) \tag{B1}$$

$$I = \frac{2a}{\omega^2} \sin \frac{\omega T}{2} \left(\cos \frac{\omega T}{2} - 1 \right) \tag{B2}$$

The magnitude of the transformation is then

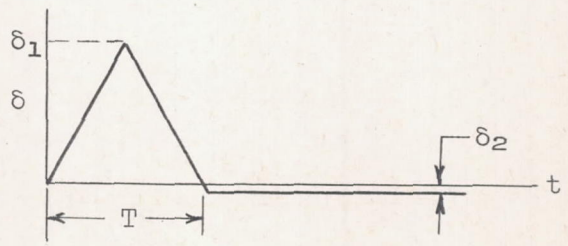
$$|\delta| = \frac{2a}{\omega^2}\left(1 - \cos\frac{\omega T}{2}\right)$$

It can be seen that $|\delta|$ is periodic and is zero when $\omega = 4\pi/T$, $8\pi/T$, ... At these frequencies the transform of the response to this input would also be zero, and thus the ratio of output to input would be indeterminate. A reduction in T would increase the period and reduce the number of indeterminate points. This is shown in figure 10 where the transform magnitudes of two triangular pulses are plotted. One has $T = 1$ second and $a = 4$, while the other has $T = 1/2$ and $a = 16$. The areas under the two triangles are equal so that their transforms have equal magnitudes at zero frequency. Reducing T from 1 second to 1/2 second doubles the period and moves the first indeterminate point from a frequency of 4π radians per second to 8π. For purposes of comparison, transformations of a unit step and a unit impulse are also shown.

As T is further reduced, the magnitude of the triangular pulse more closely approaches the constant value that is characteristic of the pure impulse. To gain full advantage from the smaller T, the slope must be increased to maintain the same area under the pulse. A practical limitation is fixed by the maximum rate at which a control surface can be moved, and any further reduction in T results in smaller over-all magnitudes. The most desirable input, therefore, is a compromise between large area and short time duration.

From figure 10 it would appear that a pulse-type input is well suited for determining low frequency characteristics. However, the following explanation will show that this is not true.

Generally it is impossible to return a control surface precisely to its initial position after application of a pulse input. Even if a chain stop or other device is used there is still apt to be a small residual deflection after time T as shown in the following sketch:



If δ_2 is exactly zero, then as ω approaches zero (from equations (B1) and (B2))

$$I \longrightarrow 0$$

$$R \longrightarrow \frac{aT^2}{4}$$

Now if δ_2 is finite, the real and imaginary parts of the transform of the entire input are

$$I = \frac{2a}{\omega^2} \sin \frac{\omega T}{2} \left(\cos \frac{\omega T}{2} - 1 \right) - \frac{\delta_2}{\omega} \cos \omega T$$

$$R = \frac{2a}{\omega^2} \cos \frac{\omega T}{2} \left(1 - \cos \frac{\omega T}{2} \right) - \frac{\delta_2}{\omega} \sin \omega T$$

In this case as $\omega \longrightarrow 0$,

$$I \longrightarrow \infty$$

$$R \longrightarrow \frac{aT^2}{4} - \delta_2 T$$

thus the zero frequency magnitude is infinitely large regardless of how small δ_2 may be. Therefore, even though δ_2 appears to be zero on a flight record (i.e., δ_2 is less than the least count of the recording instrument) there is still the possibility of an infinite error at zero frequency. A step input is not subject to these large low frequency errors; an error of 1 percent in the reading of the step deflection merely means an error of 1 percent in the transformation.

APPENDIX C

PREDICTED AIRPLANE RESPONSES

EQUATIONS OF MOTION

The three equations that define the lateral and directional motions of an airplane with respect to stability axes such as developed in reference 10 may be written as:

$$\left(I_X D^2 - qSb\, C_{l_p} \frac{b}{2V} D\right)\varphi + \left(-I_{XZ} D^2 - qSb\, C_{l_r} \frac{b}{2V} D\right)\psi - qSb\, C_{l_\beta}\beta = qSb\, C_{l_\delta}\delta \tag{C1}$$

$$\left(-I_{XZ} D^2 - qSb\, C_{n_p} \frac{b}{2V} D\right)\varphi + \left(I_Z D^2 - qSb\, C_{n_r} \frac{b}{2V} D\right)\psi - qSb\, C_{n_\beta}\beta = qSb\, C_{n_\delta}\delta \tag{C2}$$

$$(-W \cos \gamma)\varphi + (mVD - W \sin \gamma)\psi + (mVD - qSC_{Y_\beta})\beta = qSC_{Y_\delta}\delta \tag{C3}$$

By dividing equation (C1) by I_X, equation (C2) by I_Z, equation (C3) by mV, and by introducing new symbols, the three equations can be written in the more convenient form that follows:

$$(D^2 - L_p D)\varphi + (-r_X D^2 - L_r D)\psi - L_\beta \beta = L_\delta \delta \tag{C4}$$

$$(-r_Z D^2 - N_p D)\varphi + (D^2 - N_r D)\psi - N_\beta \beta = N_\delta \delta \tag{C5}$$

$$-K_1 \varphi + (D - K_2)\psi + (D - Y_\beta)\beta = Y_\delta \delta \tag{C6}$$

CHARACTERISTIC EQUATION

The characteristic equation Δ is formed by expanding the major determinant to give

$$\Delta = D(C_4 D^4 + C_3 D^3 + C_2 D^2 + C_1 D + C_0) \tag{C7}$$

where

$$C_4 = 1 - r_X r_Z$$

$$C_3 = -L_p - N_r - Y_\beta(1 - r_X r_Z) - r_X N_p - r_Z L_r$$

$$C_2 = (N_r + r_Z L_r)Y_\beta + (L_p + r_X N_p)Y_\beta + (L_p N_r - N_p L_r) + (N_\beta + r_Z L_\beta)$$

$$C_1 = -(L_p N_r - N_p L_r)Y_\beta + (L_\beta N_p - N_\beta L_p) - K_1(L_\beta + r_X N_\beta) - K_2(N_\beta + r_Z L_\beta)$$

$$C_0 = -K_1(L_r N_\beta - N_r L_\beta) - K_2(L_\beta N_p - N_\beta L_p)$$

These coefficients can be further simplified by making the following substitutions:

Let

$$L_p' = L_p + r_X Y_p \qquad N_r' = N_r + r_Z L_r$$
$$L_\beta' = L_\beta + r_X Y_\beta \qquad N_\beta' = N_\beta + r_Z L_\beta$$

Then the coefficients of the characteristic equation are finally expressed as

$$C_4 = 1 - r_X r_Z$$

$$C_3 = -L_p' - N_r' - Y_\beta(1 - r_X r_Z)$$

$$C_2 = (N_r' + L_p')Y_\beta + (L_p N_r - N_p L_r) + N_\beta'$$

$$C_1 = -(L_p N_r - N_p L_r)Y_\beta + (L_\beta N_p - N_\beta L_p) - K_1 L_\beta' - K_2 N_\beta'$$

$$C_0 = -K_1(L_r N_\beta - N_r L_\beta) - K_2(L_\beta N_p - N_\beta L_p)$$

In factored form, equation (C7) is

$$\Delta = D(D - \lambda_1)(D - \lambda_2)(D - \lambda_3)(D - \lambda_4)$$

where λ_1 and λ_2 are designated as the spiral and rolling roots, respectively, and where λ_3 and λ_4 are a complex pair $(\sigma \pm i\omega_1)$ that describe the oscillatory mode.

For convenience in this investigation Δ has been expressed as

$$\Delta = D(D - \lambda_1)(D - \lambda_2)(D^2 + c_1 D + c_2)$$

where

$$c_1 = -(\lambda_3 + \lambda_4) = -2\sigma$$

$$c_2 = \lambda_3\lambda_4 = \sigma^2 + \omega_1^2$$

Here c_1 and c_2 are real coefficients that define the damping and period of the oscillatory motion.

The quadratic term may also be written in the form

$$\omega_n^2 \left(1 + 2\zeta\frac{D}{\omega_n} + \frac{D^2}{\omega_n^2}\right)$$

where

$$\omega_n = \sqrt{c_2}$$

and

$$\zeta = \frac{c_1}{2\omega_n}$$

SIMPLIFICATIONS OF THE CHARACTERISTIC EQUATION

In the special case when the flight-path angle γ is zero and when the product of inertia is very small, it is often possible to neglect C_O and, by neglecting other small terms, the characteristic equation may be written as

$$\Delta = D^2\left[D^3 - (L_p + N_r + Y_\beta)D^2 + (L_pY_\beta + L_pN_r + N_\beta)D - L_pN_\beta\right]$$

The cubic term can be factored exactly so that

$$\Delta = D^2(D - L_p)\left[D^2 - (N_r + Y_\beta)D + N_\beta\right]$$

This form of the characteristic equation considers only the oscillatory and rolling modes. It enables the coefficients C_1, C_2, and C_3 to be expressed directly in terms of aerodynamic derivatives or simple combinations thereof.

Even when the product of inertia is significant the characteristic equation may be factored approximately into the comparable simple form

$$\Delta = D^2(D - L_p)\left[D^2 - (N_r + Y_\beta)D + N_\beta'\right]$$

While the factorization is not exact, it is nevertheless justifiable in many cases.

TRANSFER FUNCTIONS

From the three equations of motion the airplane responses in φ, ψ, and β can be readily calculated. In the following equations, δ refers to either an aileron or a rudder disturbance.

$$\frac{\varphi}{\delta} = \frac{A_3D^3 + A_2D^2 + A_1D + A_0}{\Delta}$$

where

$$A_3 = L_\delta + r_X N_\delta$$

$$A_2 = -L_\delta(Y_\beta + N_r) + N_\delta(L_r - r_X Y_\beta) + Y_\delta L_\beta'$$

$$A_1 = L_\delta(N_r Y_\beta + N_\beta) - N_\delta(L_\beta + L_r Y_\beta) + Y_\delta(L_r N_\beta - N_r L_\beta)$$

$$A_0 = K_2(N_\delta L_\beta - N_\beta L_\delta)$$

$$\frac{\psi}{\delta} = \frac{B_3D^3 + B_2D^2 + B_1D + B_0}{\Delta}$$

where

$$B_3 = N_\delta + r_Z L_\delta$$

$$B_2 = -N_\delta(L_p + Y_\beta) + L_\delta(N_p - r_Z Y_\beta) + Y_\delta N_\beta'$$

$$B_1 = N_\delta L_p Y_\beta - L_\delta N_p Y_\beta + Y_\delta(L_\beta N_p - N_\beta L_p)$$

$$B_0 = K_1(L_\delta N_\beta - N_\delta L_\beta)$$

$$\frac{\beta}{\delta} = \frac{D(E_3D^3 + E_2D^2 + E_1D + E_0)}{\Delta}$$

where

$$E_3 = Y_\delta(1 - r_X r_Z)$$

$$E_2 = -Y_\delta(N_r' + L_p') - L_\delta r_Z - N_\delta$$

$$E_1 = Y_\delta(L_p N_r - N_p L_r) - L_\delta(N_p - r_Z K_2 - K_1) + N_\delta(r_X K_1 + L_p + K_2)$$

$$E_0 = K_1(N_\delta L_r - L_\delta N_r) + K_2(L_\delta N_p - N_\delta L_p)$$

Simplifications can also be made in these expressions by neglecting small quantities; however, this can be shown more clearly in the numerical example that follows.

NUMERICAL EXAMPLE AT M = 0.8

Using values of stability derivatives shown in table II, and with $\gamma = 0$, predicted responses for $p = D\varphi$, $r = D\psi$, and β for both aileron and rudder inputs have been calculated and found to be

$$\Delta = D(D^4 + 3.652D^3 + 15.16D^2 + 41.26D + 0.0289)$$

$$= D(D + 0.00070)\ (D + 3.078)\ (D^2 + 0.573D + 13.40)$$

$$\frac{r}{\delta_r} = \frac{-7.60D(D + 3.091)\ (D^2 + 0.0270D + 0.208)}{\Delta}$$

$$\frac{p}{\delta_r} = \frac{5.16D^2(D + 4.436)\ (D - 5.210)}{\Delta}$$

$$\frac{\beta}{\delta_r} = \frac{0.0339D(D + 3.053)\ (D + 225.3)\ (D - 0.00703)}{\Delta}$$

$$\frac{r}{\delta_a} = \frac{0.699D(D + 3.978)\ (D^2 - 1.758D + 7.358)}{\Delta}$$

$$\frac{p}{\delta_a} = \frac{36.4D^2(D^2 + 0.655D + 13.68)}{\Delta}$$

$$\frac{\beta}{\delta_a} = \frac{0.0008D(D + 0.990)\ (D - 1.094)\ (D - 870)}{\Delta}$$

By neglecting small terms, r/δ_r can be expressed as

$$\frac{r}{\delta_r} = \frac{-7.60D^3(D + 3.091)}{D^2(D + 3.078)\ (D^2 + 0.573D + 13.40)}$$

and then by an approximate cancellation this reduces to

$$\frac{r}{\delta_r} = \frac{-7.60D}{D^2 + 0.573D + 13.40}$$

Similarly, β/δ_r can be simplified by neglecting small terms so that

$$\frac{\beta}{\delta_r} = \frac{7.64D^2(D + 3.053)}{D^2(D + 3.078)\ (D^2 + 0.573D + 13.40)} \approx \frac{7.64}{D^2 + 0.573D + 13.40}$$

It can be seen that this expression for β/δ_r is practically indentical (with opposite sign) to the integral of the simplified equation for r/δ_r. It is also possible to simplify p/δ_a as follows:

$$\frac{p}{\delta_a} = \frac{36.4D^2(D^2 + 0.655D + 13.68)}{D^2(D + 3.078)\ (D^2 + 0.573D + 13.40)} \approx \frac{36.4}{D + 3.078}$$

Similar simplifications have been made for other Mach numbers and found to be equally valid.

APPENDIX D

FLIGHT EVALUATION OF C_{l_β}

From time histories of the free oscillatory responses of p and r it is possible to evaluate the derivative C_{l_β} provided the derivatives C_{n_β} and C_{l_p} are known. The method employed is explained in some detail in reference 5 and is briefly summarized here.

When the three equations of motion are set equal to zero and written in determinant form, expansion of the appropriate minor determinants about the third row yields cofactors of φ and ψ.

The cofactor of φ, C_φ is

$$C_\varphi = (r_X D^2 + L_r D)N_\beta + (D^2 - N_r D)L_\beta$$
$$= D\left[L_\beta' D + (L_r N_\beta - N_r L_\beta)\right]$$

The quantity $L_r N_\beta - N_r L_\beta$ is generally very small and C_φ can be closely approximated as

$$C_\varphi = L_\beta' D^2$$

The cofactor of ψ, C_ψ is

$$C_\psi = -(D^2 - L_p D)N_\beta - (r_Z D^2 + N_p D)L_\beta$$
$$= -D\left[N_\beta' D - (L_p N_\beta - N_p L_\beta)\right]$$

In this case the term $N_p L_\beta$ is small compared to $L_p N_\beta$ and the expression for C_ψ can be approximated as

$$C_\psi = -DN_\beta'(D - L_p)$$

The ratio of the two cofactors is then

$$\frac{C_\varphi}{C_\psi} = \frac{L_\beta' D}{-N_\beta'(D - L_p)}$$

When the complex root $\lambda_3 = \sigma + i\omega_1$ is substituted for the operator D, this expression is the ratio of the free oscillatory responses of φ and ψ at any time t. The ratio of p to r is obviously the same and can be expressed as

$$\frac{p}{r} = \frac{-L_{\beta}'(\sigma + i\omega_1)}{N_{\beta}'(\sigma + i\omega_1 - L_p)}$$

The actual magnitude of this ratio is

$$\left|\frac{p}{r}\right| = \frac{L_{\beta}' \sqrt{\sigma^2 + \omega_1^2}}{N_{\beta}' \sqrt{(\sigma - L_p)^2 + \omega_1^2}}$$

In this form $|p/r|$ is the ratio at any time t of the amplitudes of the envelopes that enclose the oscillatory motions of p and r; σ is the rate of damping of the envelope; and ω_1 is the natural frequency of oscillation. When σ is very small as compared to ω_1 it can be omitted; thus

$$\left|\frac{p}{r}\right| = \frac{L_{\beta}'\omega_1}{N_{\beta}'\sqrt{L_p^2 + \omega_1^2}} = \frac{L_{\beta}'}{N_{\beta}'\sqrt{1 + (L_p/\omega_1)^2}}$$

If N_{β}' and L_p are known, it is then possible to evaluate L_{β}' from measured time histories of p and r.

REFERENCES

1. Triplett, William C., and Smith, G. Allan: Longitudinal Frequency-Response Characteristics of a 35° Swept-Wing Airplane as Determined From Flight Measurements, Including a Method for the Evaluation of Transfer Functions. NACA RM A51G27, 1951.

2. Thompson, Jim Rogers, Bray, Richard S., and Cooper, George E.: Flight Calibration of Four Airspeed Systems on a Swept-Wing Airplane at Mach Numbers up to 1.04 by the NACA Radar-Phototheodolite Method. NACA RM A50H24, 1950.

3. Lees, Sidney: Graphical Aids for the Graphical Representation of Functions of the Imaginary Argument. M.I.T., Instrumentation Lab., Engineering Memo. E-25, Feb. 1951.

4. McNeill, Walter E., and Cooper, George E.: A Comparison of the Measured and Predicted Lateral Oscillatory Characteristics of a 35° Swept-Wing Fighter Airplane. NACA RM A51C28, 1951.

5. Rosamond, D. L.: Practical Methods for Lateral Stability Analyses. McDonnell Aircraft Corp. Rep. No. 2126, 1951.

6. Rathert, George A., Jr., Rolls, L. Stewart, Winograd, Lee, and Cooper, George E.: Preliminary Flight Investigation of the Wing-Dropping Tendency and Lateral-Control Characteristics of a 35° Swept-Wing Airplane at Transonic Mach Numbers. NACA RM A50H03, 1950.

7. McFadden, Norman M., Rathert, George A., Jr., and Bray, Richard S.: The Effectiveness of Wing Vortex Generators in Improving the Maneuvering Characteristics of a Swept-Wing Airplane at Transonic Speeds. NACA RM A51J18, 1952.

8. Cole, Henry Ambrose, Jr., and Ganzer, Victor Martin: Experimental Investigation of Rolling Performance of Straight and Swept-Back Flexible Wings With Various Ailerons. NACA TN 2563, 1951.

9. Skoog, Richard B., and Brown, Harvey H.: A Method for the Determination of the Spanwise Load Distribution of a Flexible Swept Wing at Subsonic Speeds. NACA TN 2222, 1951.

10. Perkins, Courtland D., and Hage, Robert E.: Airplane Performance Stability and Control. John Wiley and Sons, Inc. N.Y., 1949.

TABLE I.- PHYSICAL CHARACTERISTICS OF TEST AIRPLANE

Wing	
Total area	287.9 sq ft
Span	37.1 ft
Aspect ratio	4.79
Taper ratio	0.51
Mean aerodynamic chord	97.03 in.
Dihedral	3°
Sweepback of quarter-chord line	35°14'
Aerodynamic and geometric twist	2°
Root airfoil section (normal to quarter-chord line)	NACA 0012-64 (modified)
Tip airfoil section (normal to quarter-chord line)	NACA 0011-64 (modified)
Ailerons	
Area, each	18.6 sq ft
Span	9.18 ft
Chord, average	2.03 ft
Deflection, maximum	14° up, 14° down
Inboard end at	51.6%b/2
Vertical tail	
Area, total	34.4 sq ft
Span	7.5 ft
Aspect ratio	1.74
Taper ratio	0.36
Sweepback of quarter-chord line	35°00'
Rudder	
Area	8.1 sq ft
Span	6.6 ft
Chord, average	1.23 ft
Deflection, maximum	24.8° right, 25° left
Average weight for calculations	12,800 lb
Moment of inertia about X axis	7,245 slug ft^2
Moment of inertia about Z axis	23,190 slug ft^2
Inclination of principal longitudinal axis with respect to fuselage reference axis	-2.5°

TABLE II.- PARAMETERS USED IN ESTIMATING AIRPLANE RESPONSES

	Altitude, 35,000 feet						Altitude, 10,000 feet			
M	0.5	0.6	0.7	0.8	0.9	1.0	0.5	0.6	0.7	0.8
V	486	583	681	778	875	972	538	646	754	862
q	87.0	125.2	170.6	222.5	281.8	347.5	254.7	366.7	499.0	652.0
C_L	.51	.36	.26	.16	.13	.12	.17	.12	.09	.07
α	7.2	5.3	3.8	2.8	2.4	1.2	2.1	1.3	.8	.4
I_{xz}	-1297	-773	-359	-83	28	386	124	331	469	580
C_{l_β}	-.1025	-.0857	-.0773	-.0741	-.0721	-.0768	-.0627	-.0573	-.0563	-.0571
C_{n_β}	.1100	.1146	.1199	.1273	.1366	.1467	.1105	.1144	.1200	.1270
C_{Y_β}	-.690	-.701	-.715	-.733	-.757	-.782	-.690	-.701	-.716	-.735
C_{l_p}	-.360	-.367	-.375	-.385	-.399	-.414	-.358	-.366	-.375	-.386
C_{n_p}	-.0328	-.0225	-.0160	-.0120	-.0092	-.0068	-.0113	-.0076	-.0055	-.0044
C_{l_r}	.157	.130	.116	.108	.106	.104	.091	.082	.078	.076
C_{n_r}	-.1820	-.1852	-.1896	-.1970	-.2065	-.2170	-.1817	-.1866	-.1922	-.1984
$C_{l_{\delta_r}}$	.0077	.0102	.0138	.0155	.0160	.0183	.0130	.0160	.0180	.0200
$C_{n_{\delta_r}}$	-.0730	-.0728	-.0725	-.0742	-.0736	-.0582	-.0729	-.0728	-.0733	-.0742
$C_{Y_{\delta_r}}$	.160	.160	.160	.160	.160	.160	.160	.160	.160	.160
$C_{l_{\delta_a}}$	.112	.114	.113	.111	.088	.043	.110	.110	.110	.110
$C_{n_{\delta_a}}$	-.0050	.0020	.0059	.0081	.0095	.0105	.0050	.0095	.0110	.0120
$C_{Y_{\delta_a}}$	.004	.004	.004	.004	.004	.004	.004	.004	.004	.004
λ_1	-.00192	-.00113	-.00076	-.00070	-.00027	-.00077	-.00144	-.00153	-.00146	-.00123
λ_2	-1.809	-2.203	-2.667	-3.078	-3.581	-4.168	-4.77	-5.87	-7.01	-8.17
c_1	.378	.438	.497	.573	.679	.740	.910	1.119	1.322	1.524
c_2	5.24	7.25	9.91	13.40	18.03	23.45	12.75	19.48	28.35	38.35

TABLE III.- EFFECTS OF N_p, L_r, I_{XZ}, AND γ ON COEFFICIENTS OF THE CHARACTERISTIC EQUATION

$[\Delta = (D - \lambda_1)(D - \lambda_2)(D^2 + c_1 D + c_2)]$

(a) Effect of variations in C_{n_p}				
N_p	Spiral root λ_1	Rolling root λ_2	Oscillatory mode	
			c_1	c_2
-0.10	-0.00168	-1.951	0.235	5.55
-.05	-.00192	-1.809	.378	5.24
0	-.00206	-1.731	.455	5.10
.05	-.00223	-1.646	.541	4.96
(b) Effect of variations in C_{l_r}				
L_r	λ_1	λ_2	c_1	c_2
1.688	0.0216	-1.818	0.393	5.30
.844	-.0019	-1.809	.378	5.24
0	-.0262	-1.804	.359	5.18
-.844	-.0520	-1.795	.342	5.12
(c) Effect of variations in I_{XZ}				
I_{XZ}	λ_1	λ_2	c_1	c_2
-2594	-0.00191	-1.680	0.608	5.86
-1297	-.00192	-1.809	.378	5.24
0	-.00193	-1.956	.176	4.78
(d) Effect of flight-path angle				
γ	λ_1	λ_2	c_1	c_2
0	-0.00192	-1.809	0.378	5.24
-30°	-.0313	-1.812	.356	5.24
-90°	-.0595	-1.816	.314	5.23



Figure 1.- Photograph of test airplane.

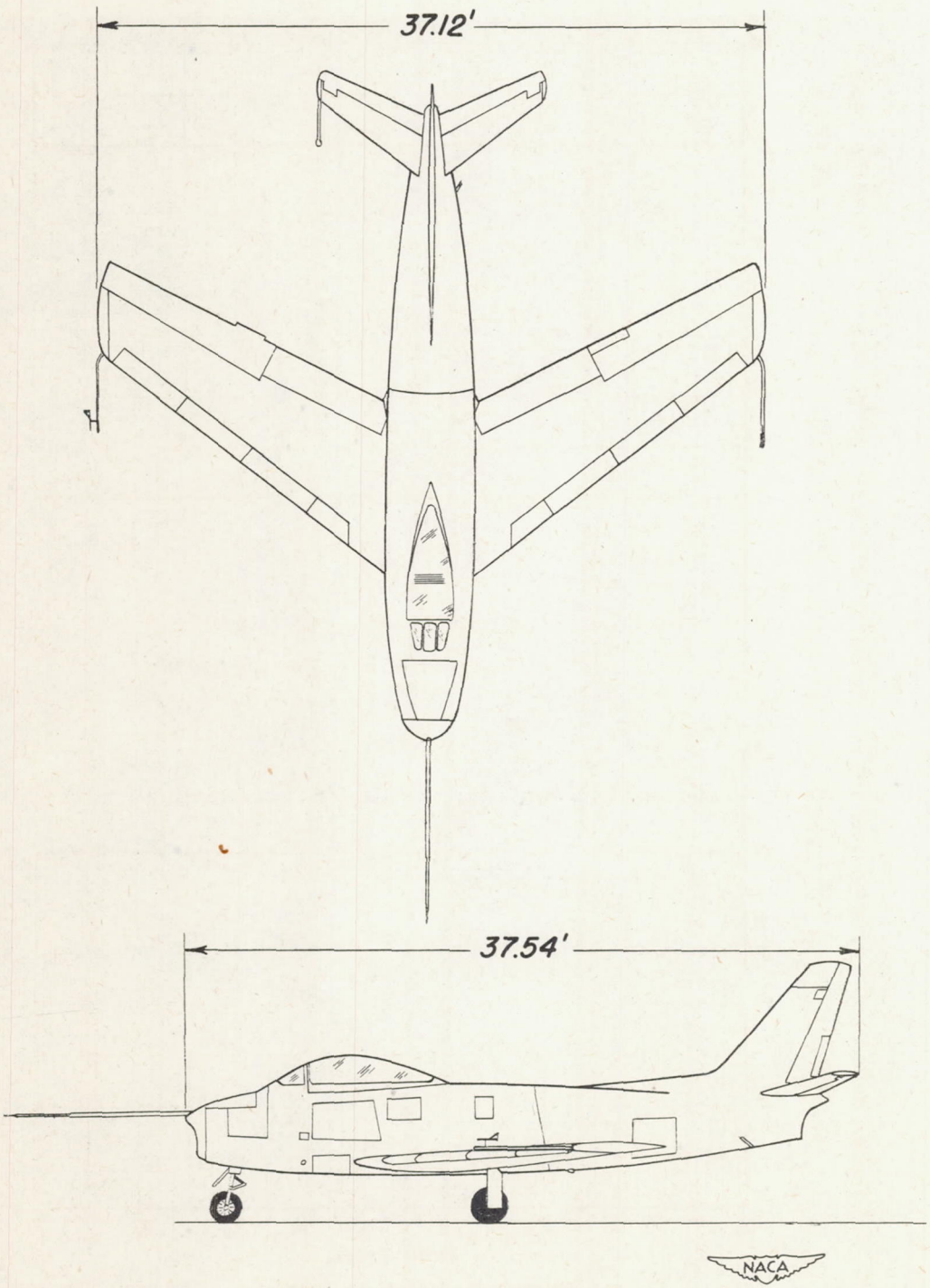
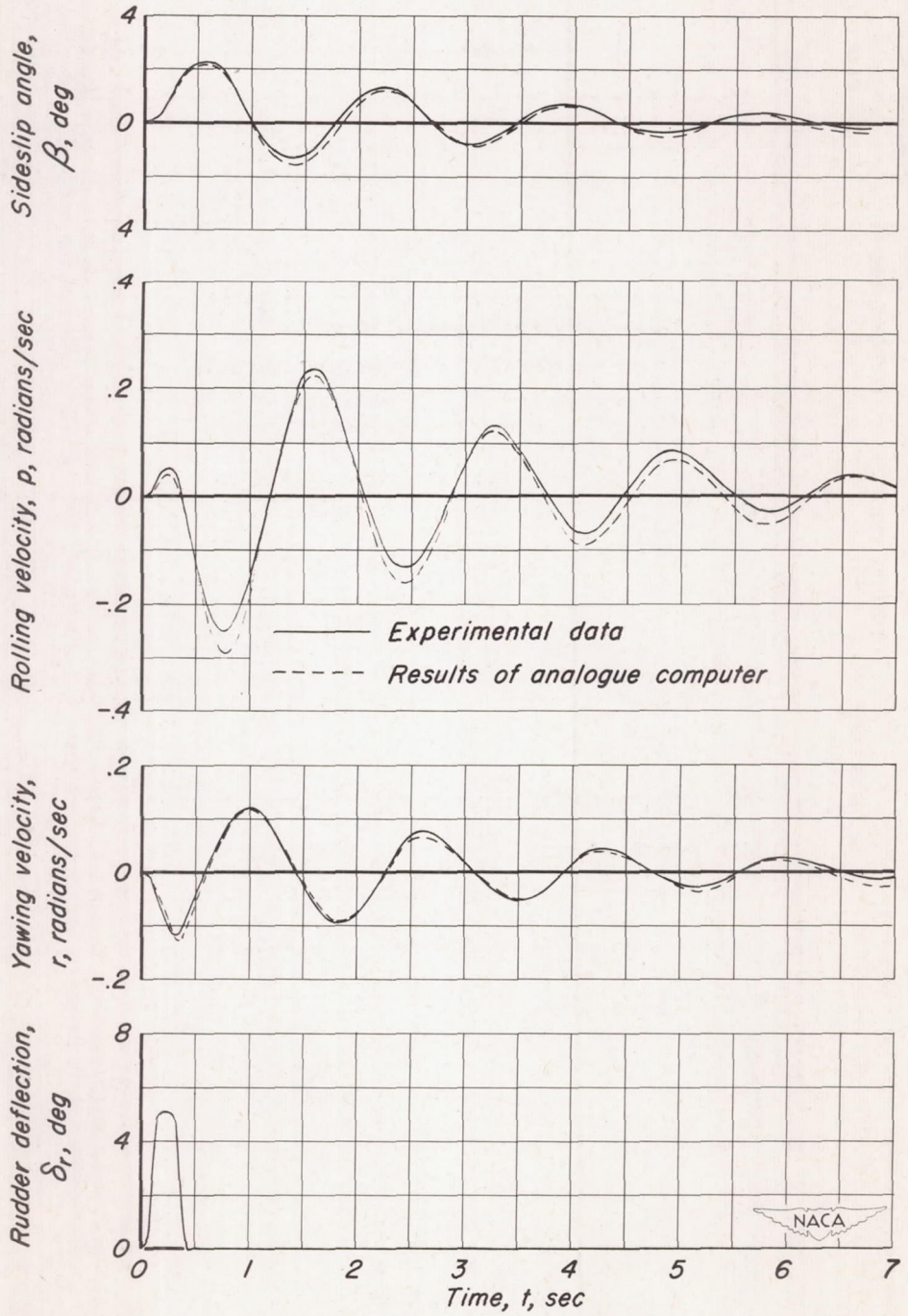
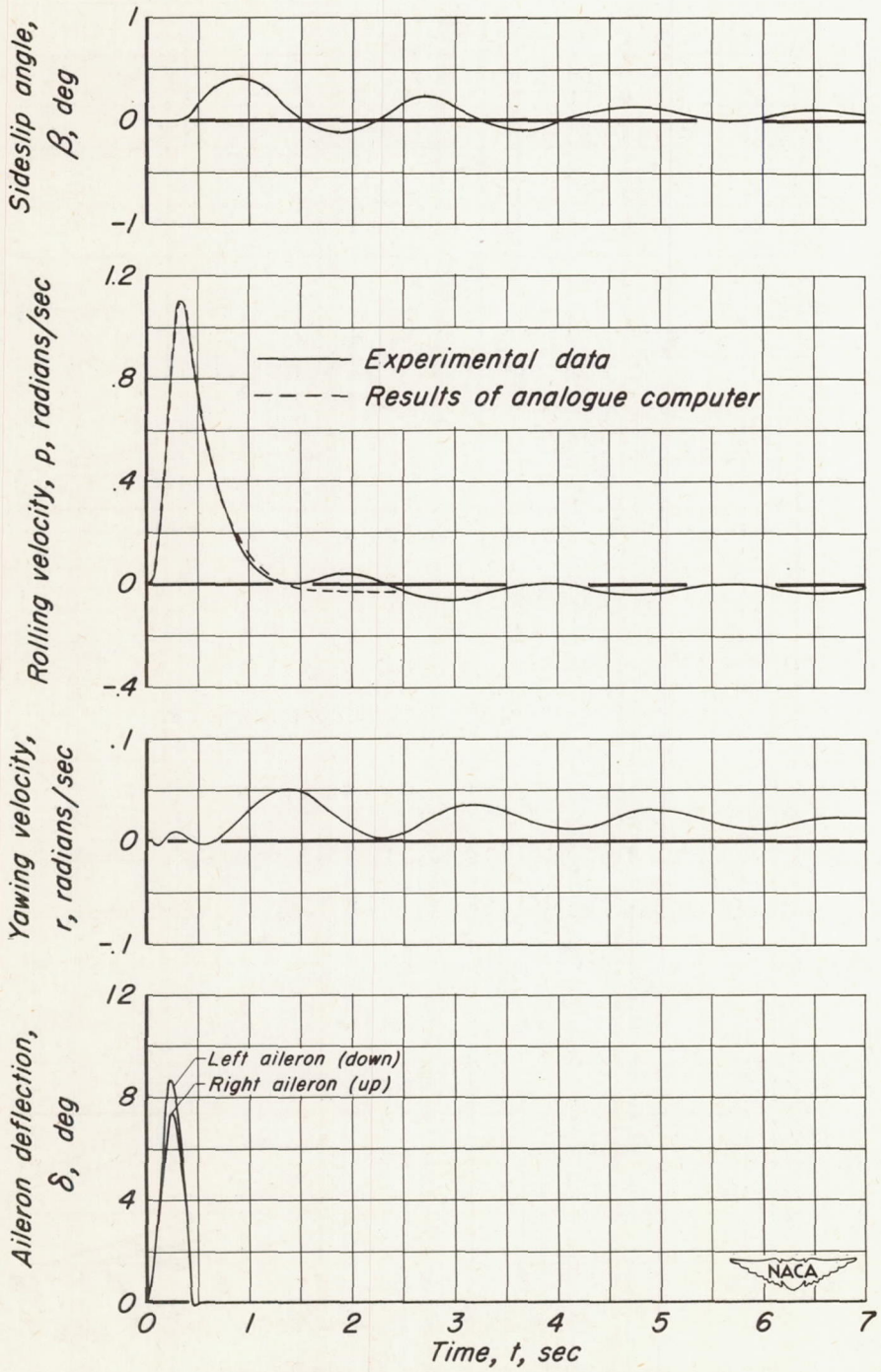


Figure 2.- Two-view drawing of the test airplane.



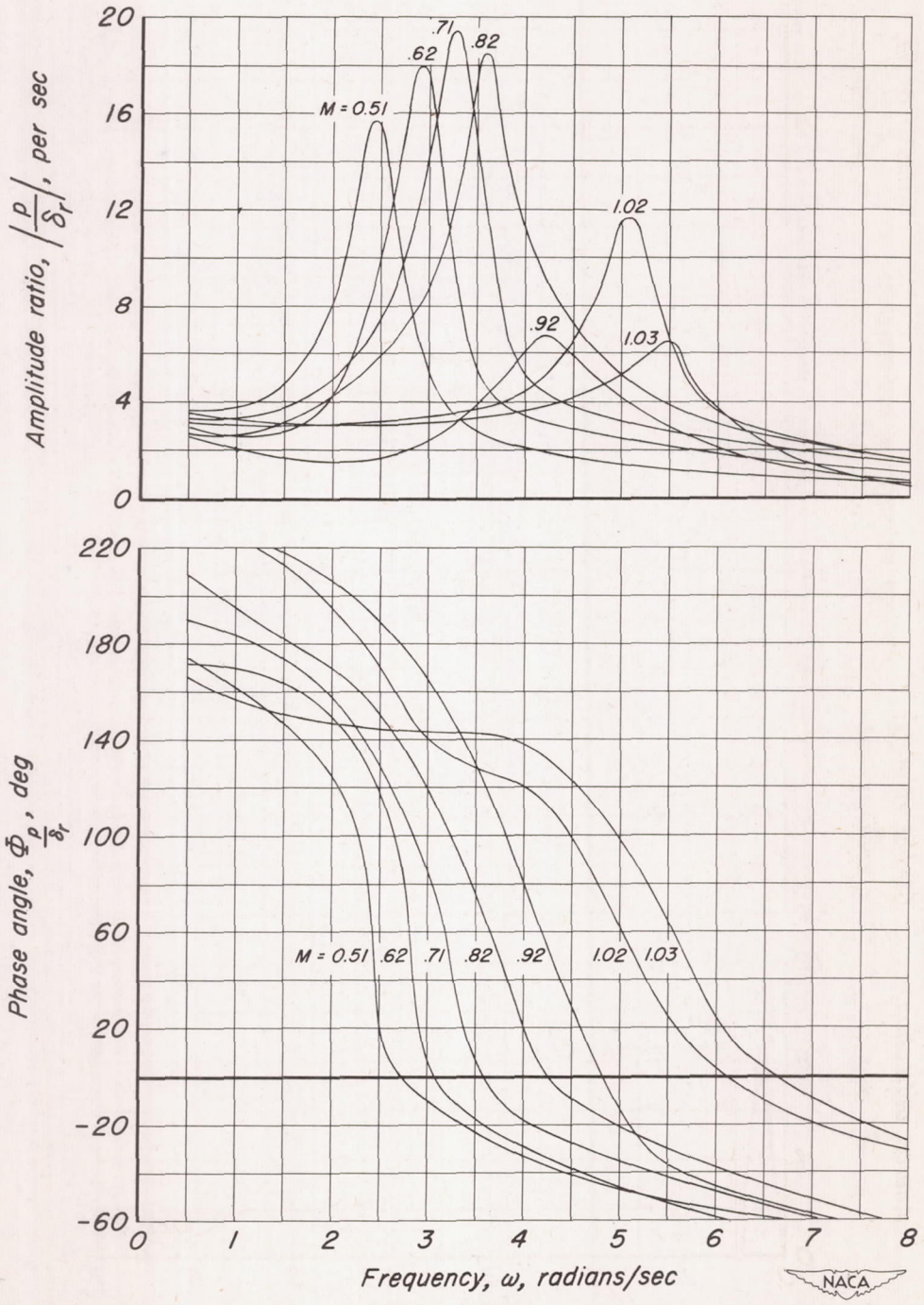
(a) Rudder pulse-type input.

Figure 3.- Sample flight records of yawing velocity, rolling velocity, and sideslip angle at a Mach number of 0.81.



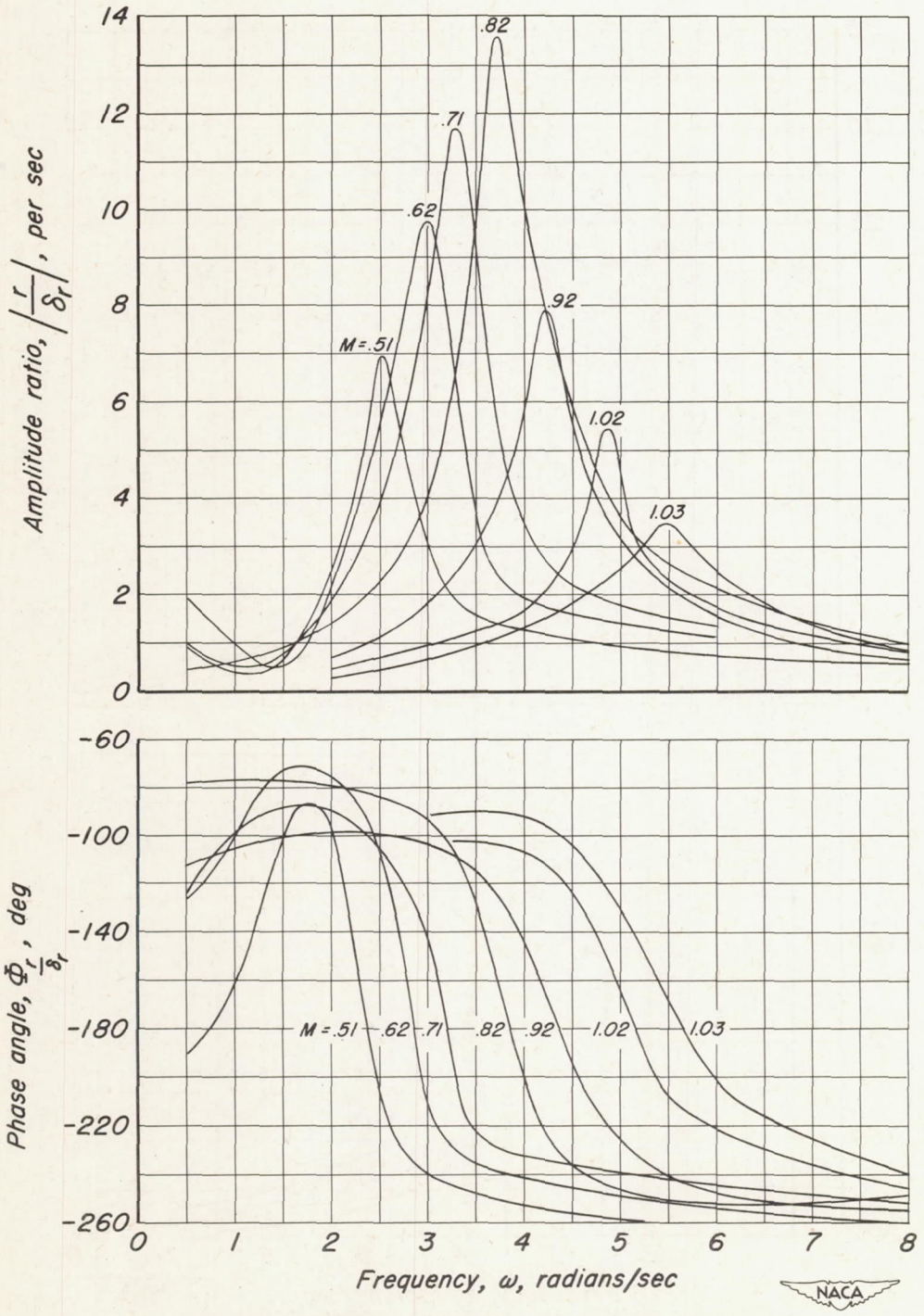
(b) Aileron pulse - type input.

Figure 3.- Concluded.



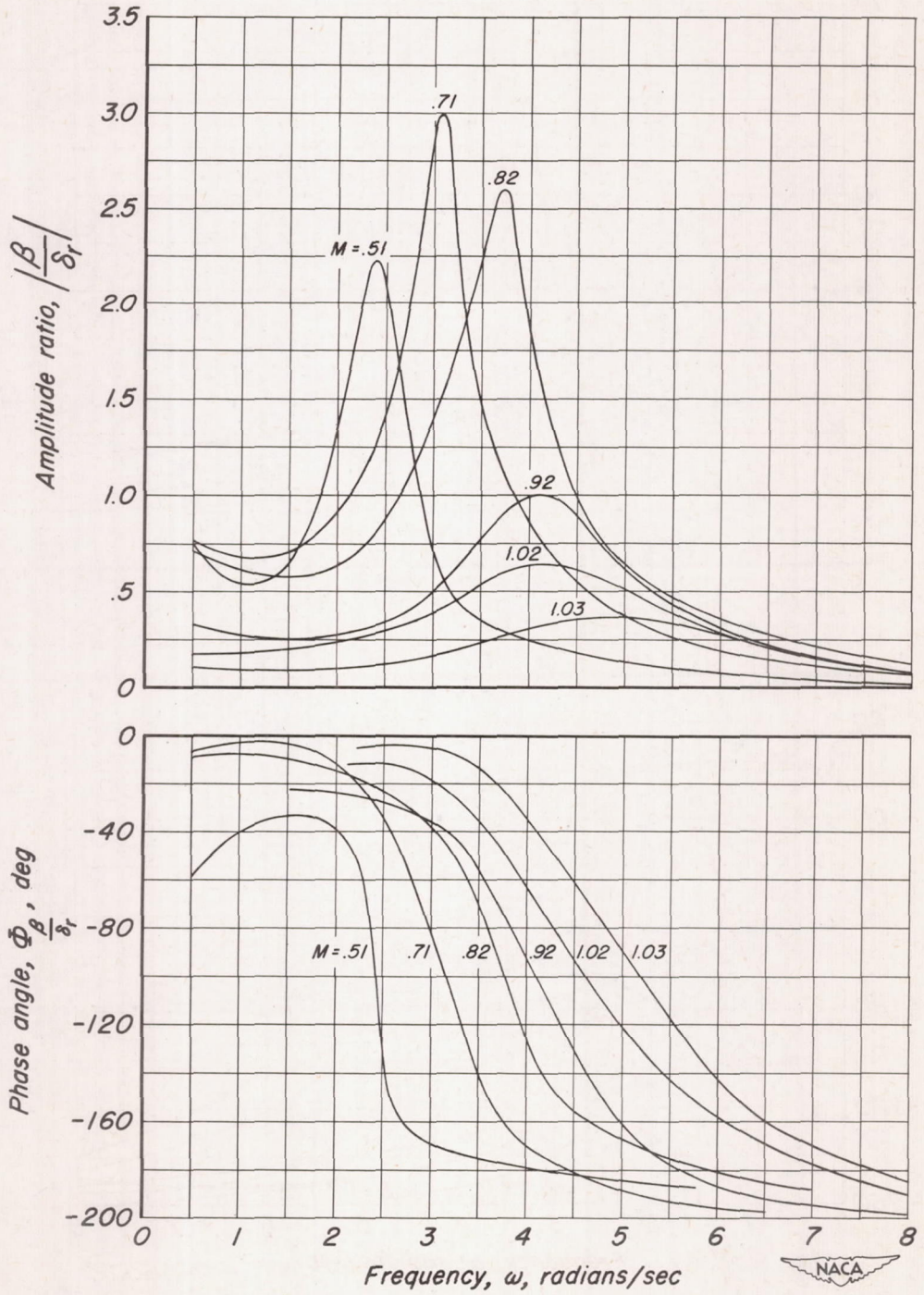
(a) Rolling velocity response to rudder input.

Figure 4.–Lateral-directional frequency responses at various flight Mach numbers at 35,000 feet.



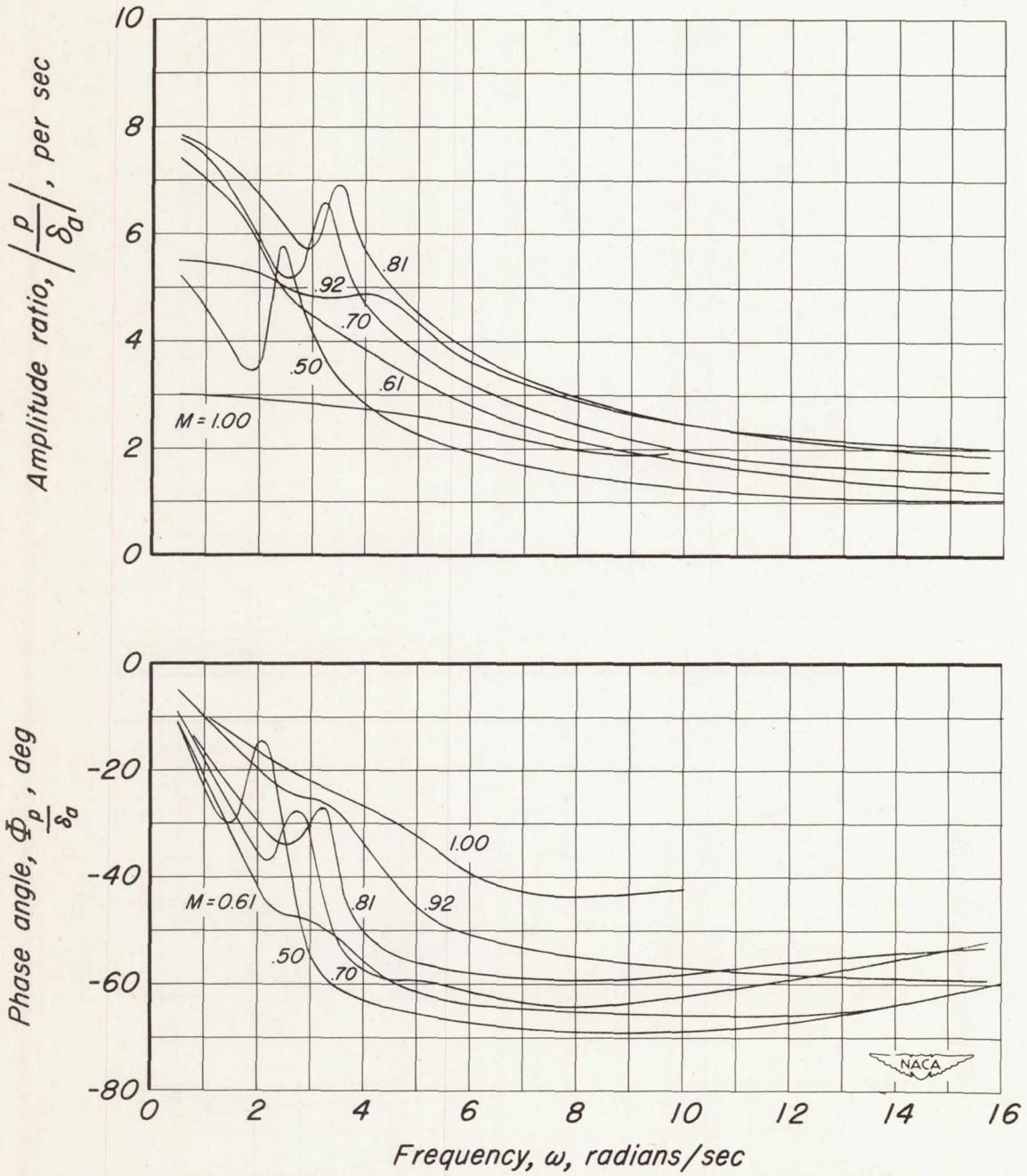
(b) Yawing velocity response to rudder input.

Figure 4.- Continued.



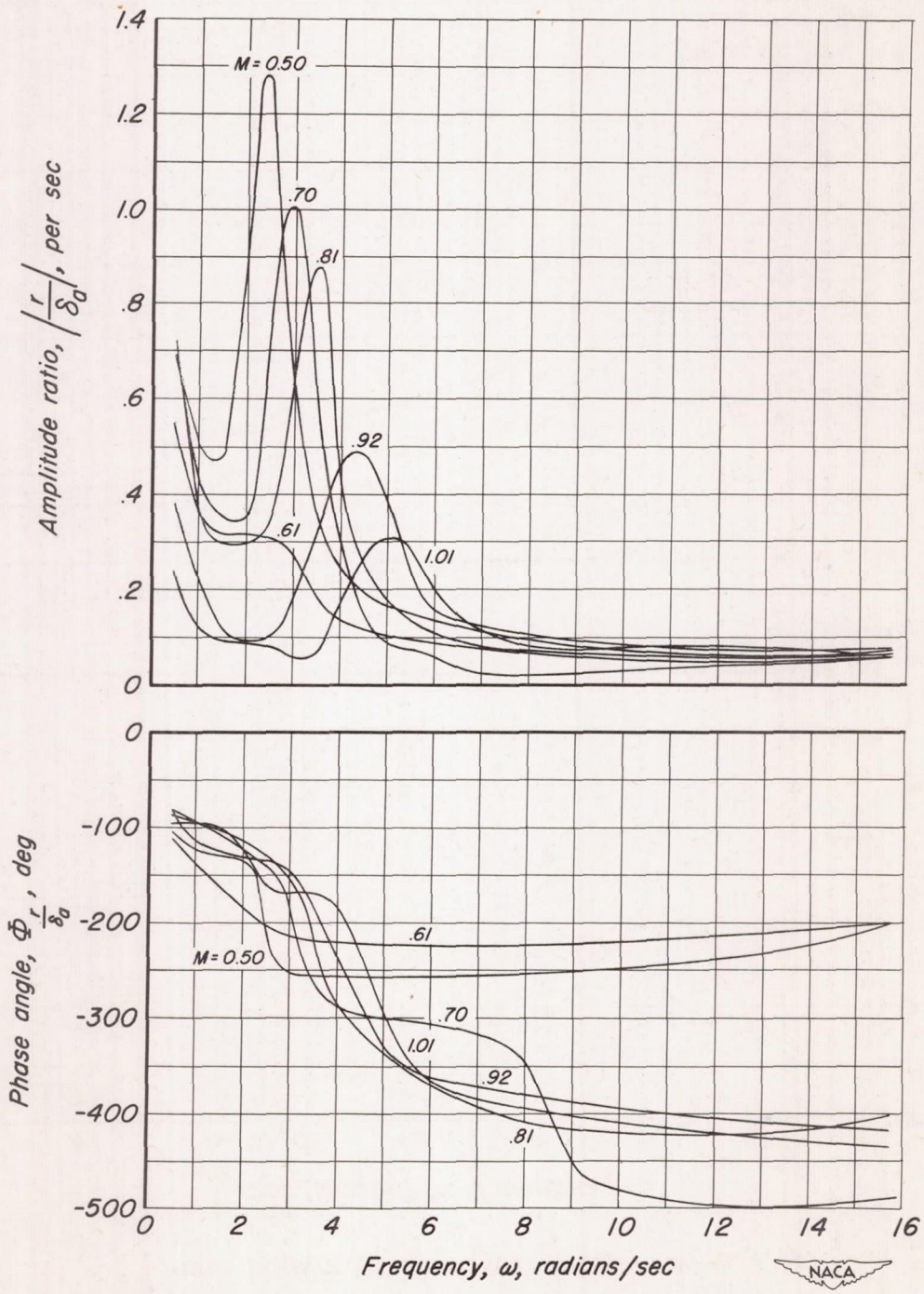
(c) Sideslip angle response to rudder input.

Figure 4.- Continued.



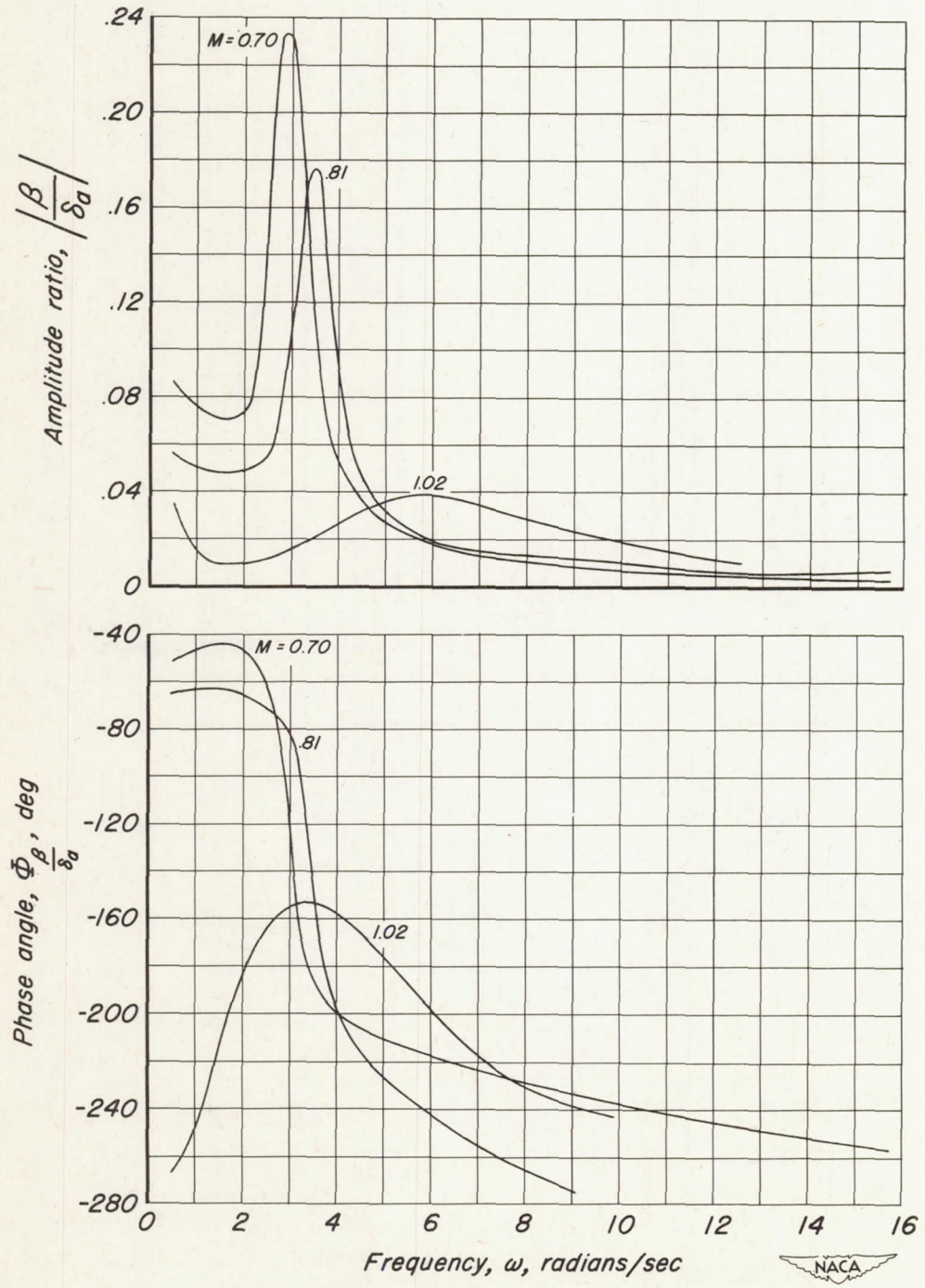
(d) Rolling velocity response to aileron input.

Figure 4.– Continued.



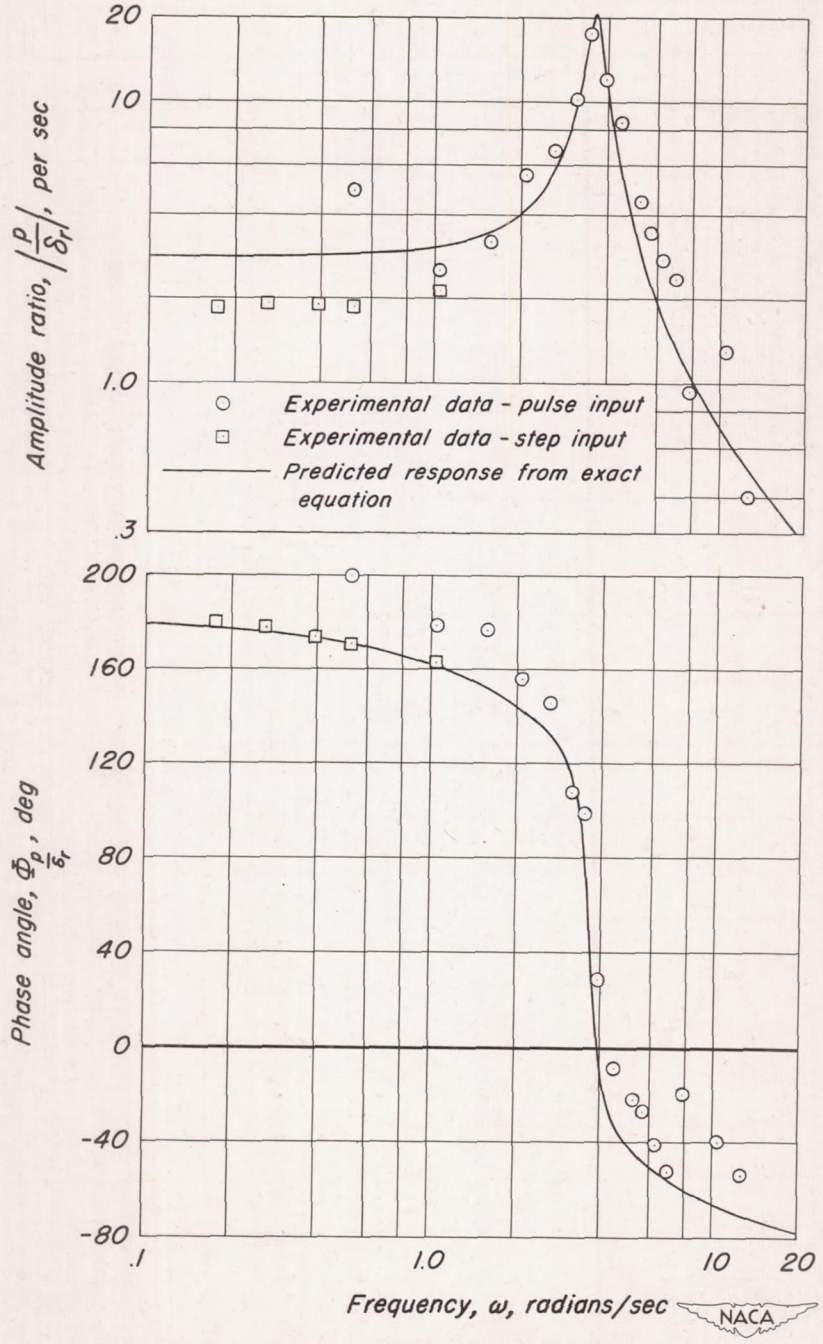
(e) Yawing velocity response to aileron input.

Figure 4.- Continued.



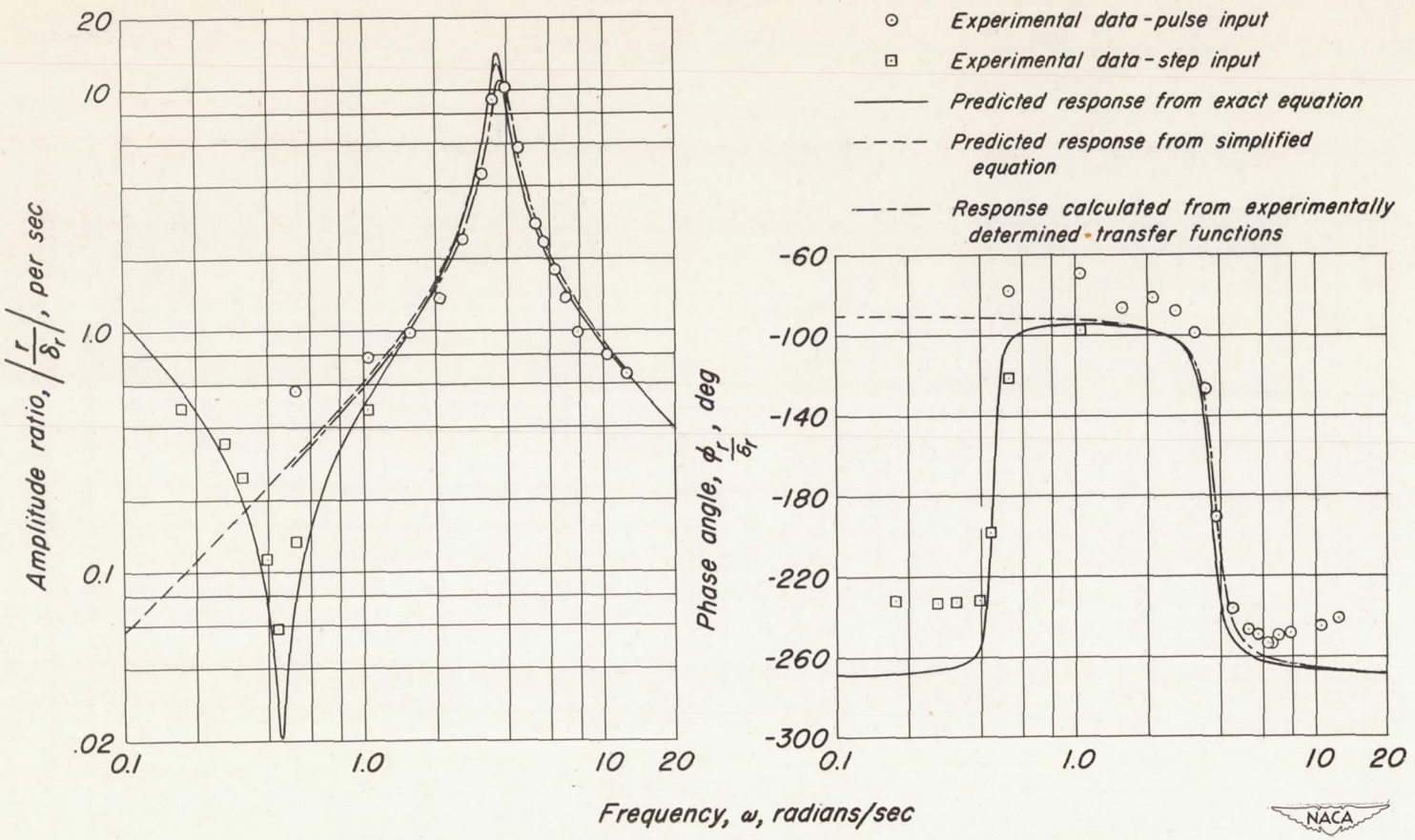
(f) Sideslip angle response to aileron input.

Figure 4.- Concluded.



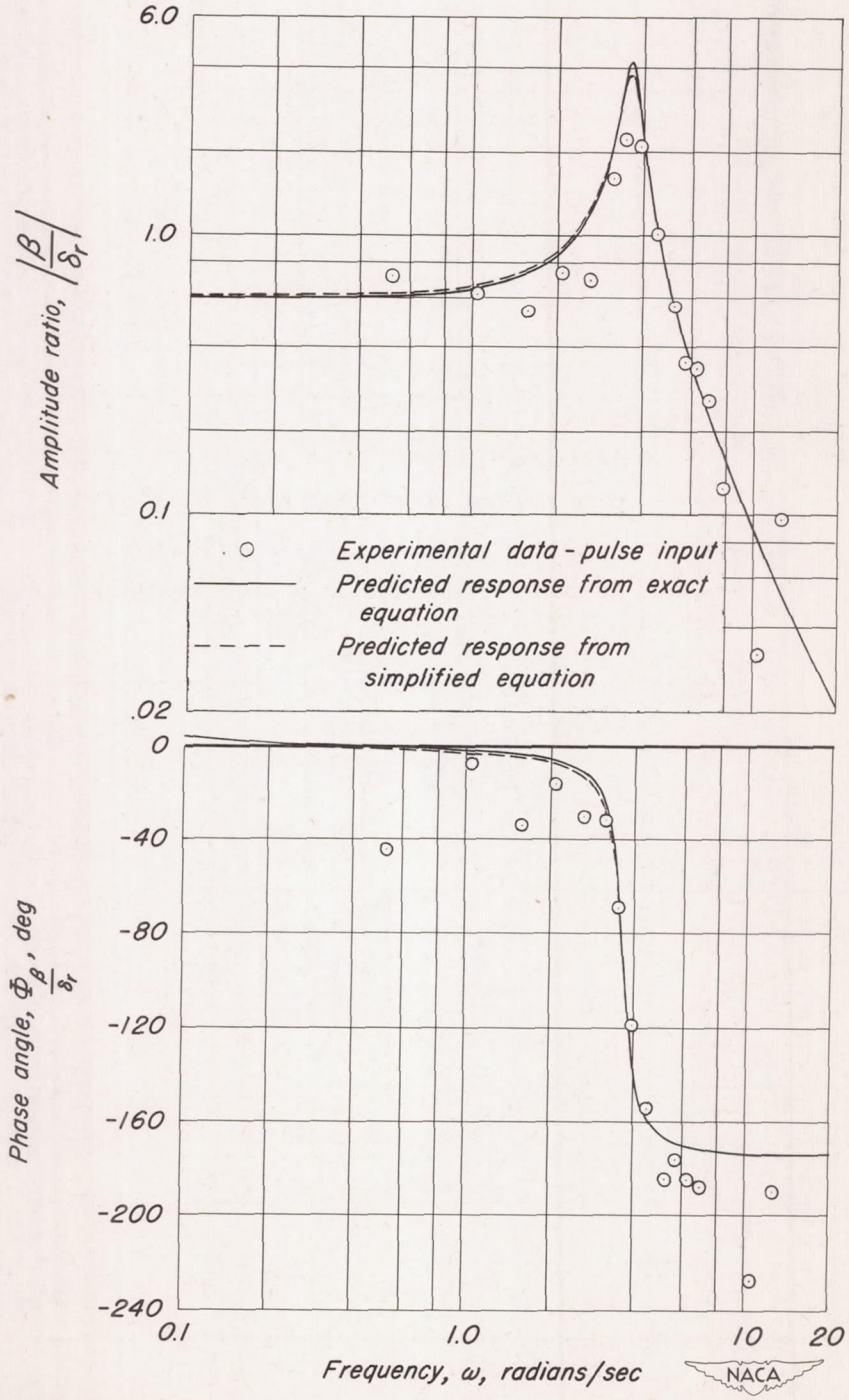
(a) Rolling velocity response to rudder input; altitude, 35,000 feet.

Figure 5.- Comparison of experimental and predicted lateral-directional frequency responses at a Mach number of 0.81.



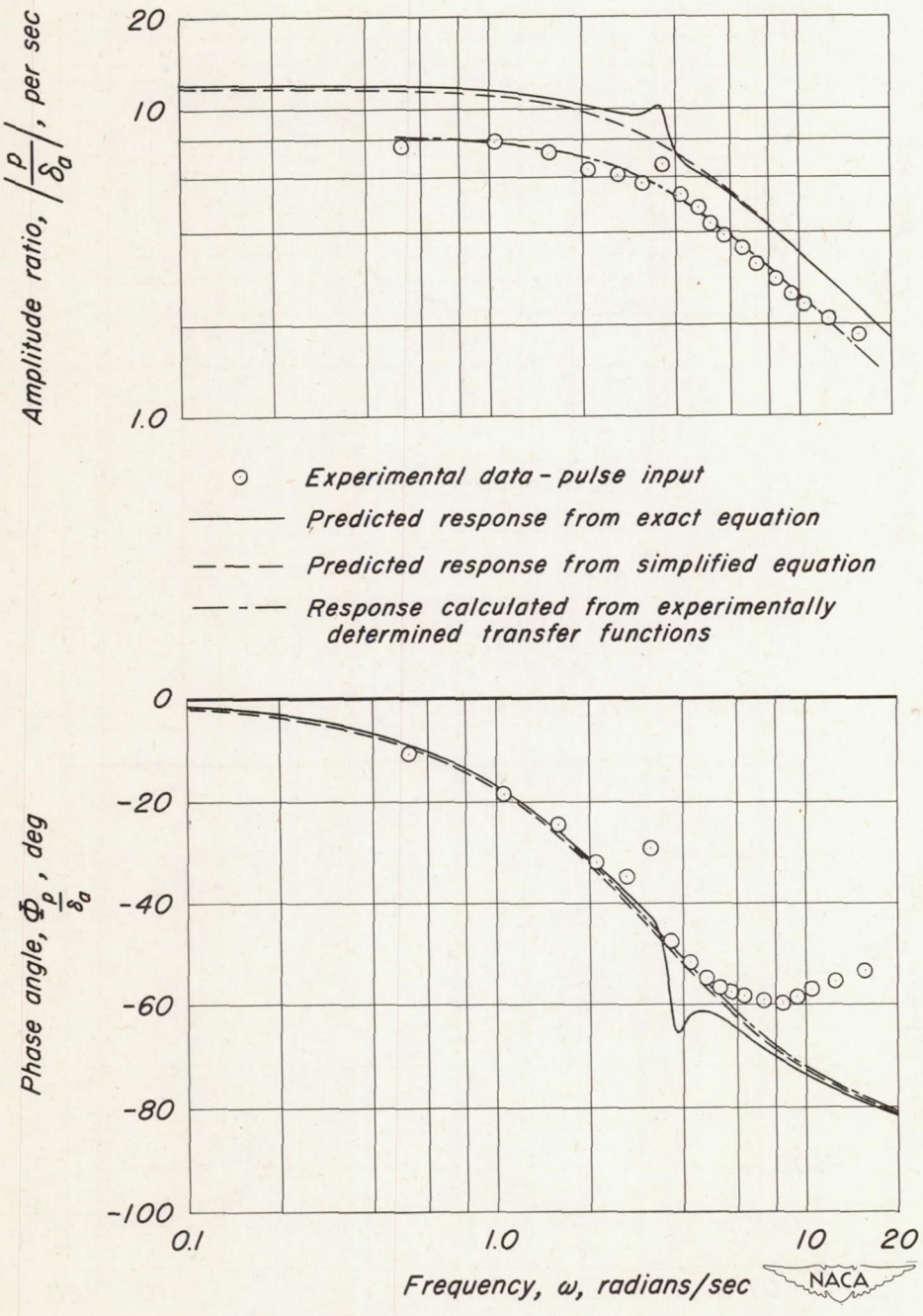
(b) Yawing velocity response to rudder input; altitude, 35,000 feet

Figure 5.- Continued.



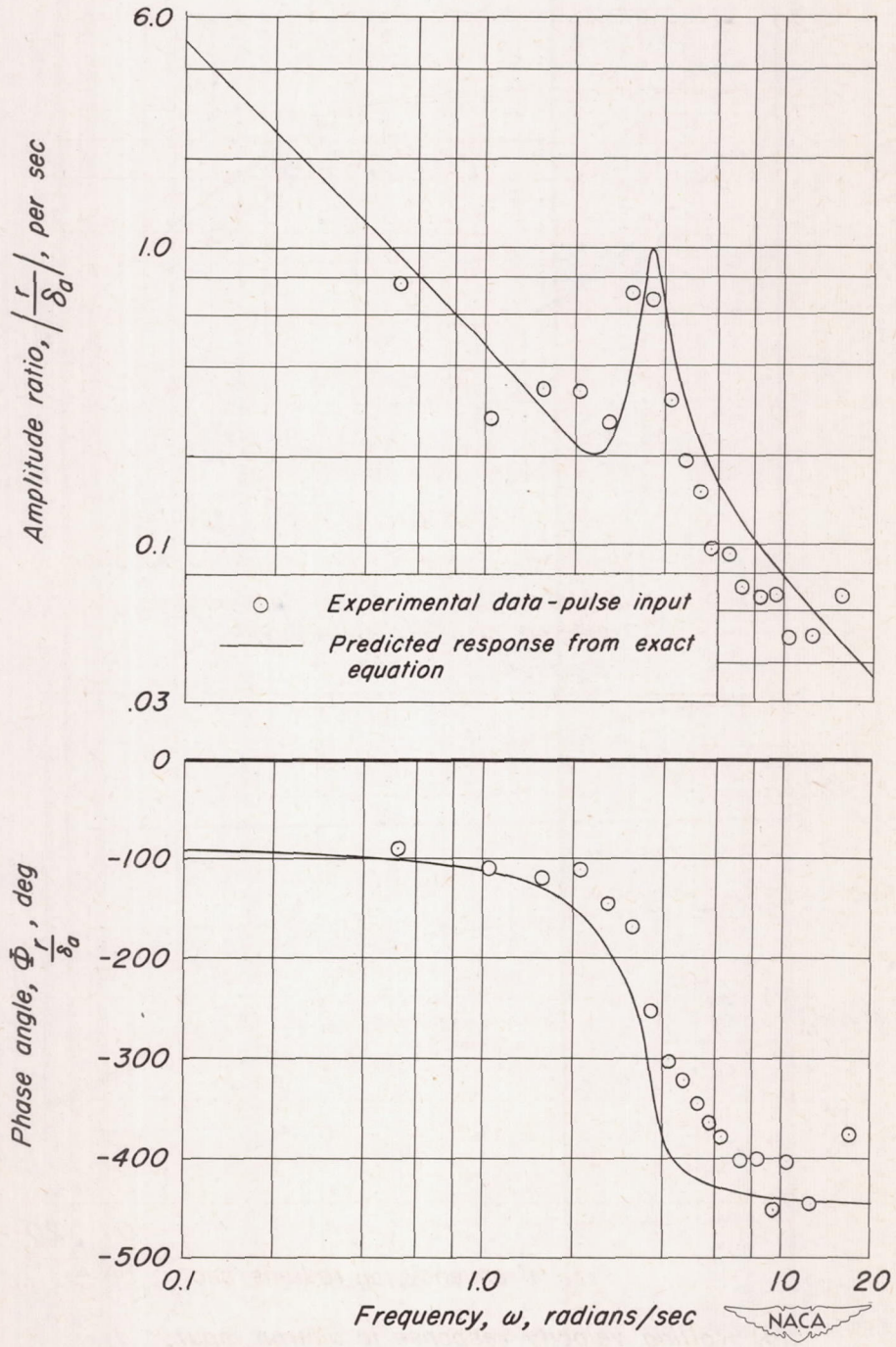
(c) Sideslip angle response to rudder input; altitude, 35,000 feet.

Figure 5.- Continued.



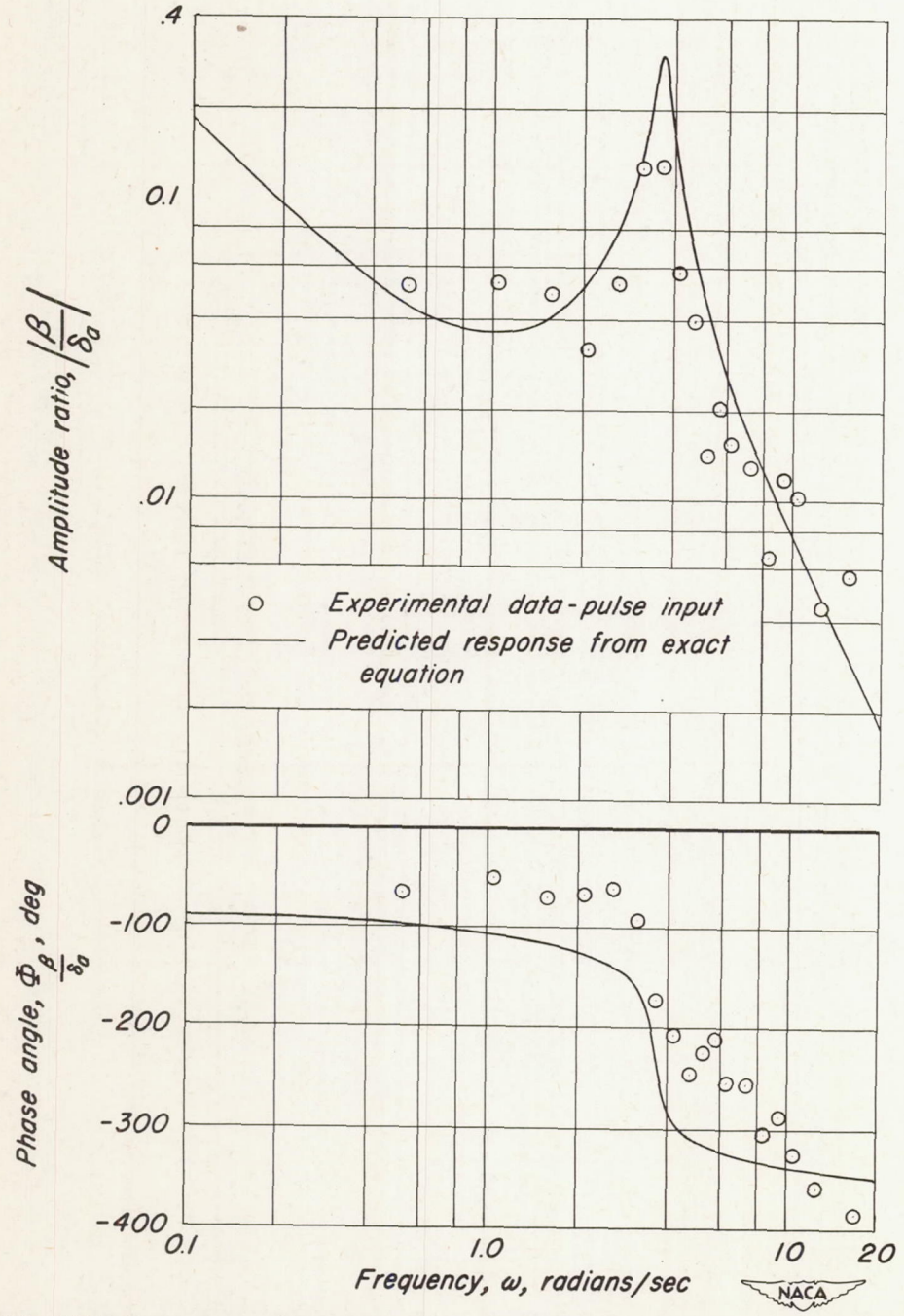
(d) Rolling velocity response to aileron input; altitude, 35,000 feet.

Figure 5.- Continued.



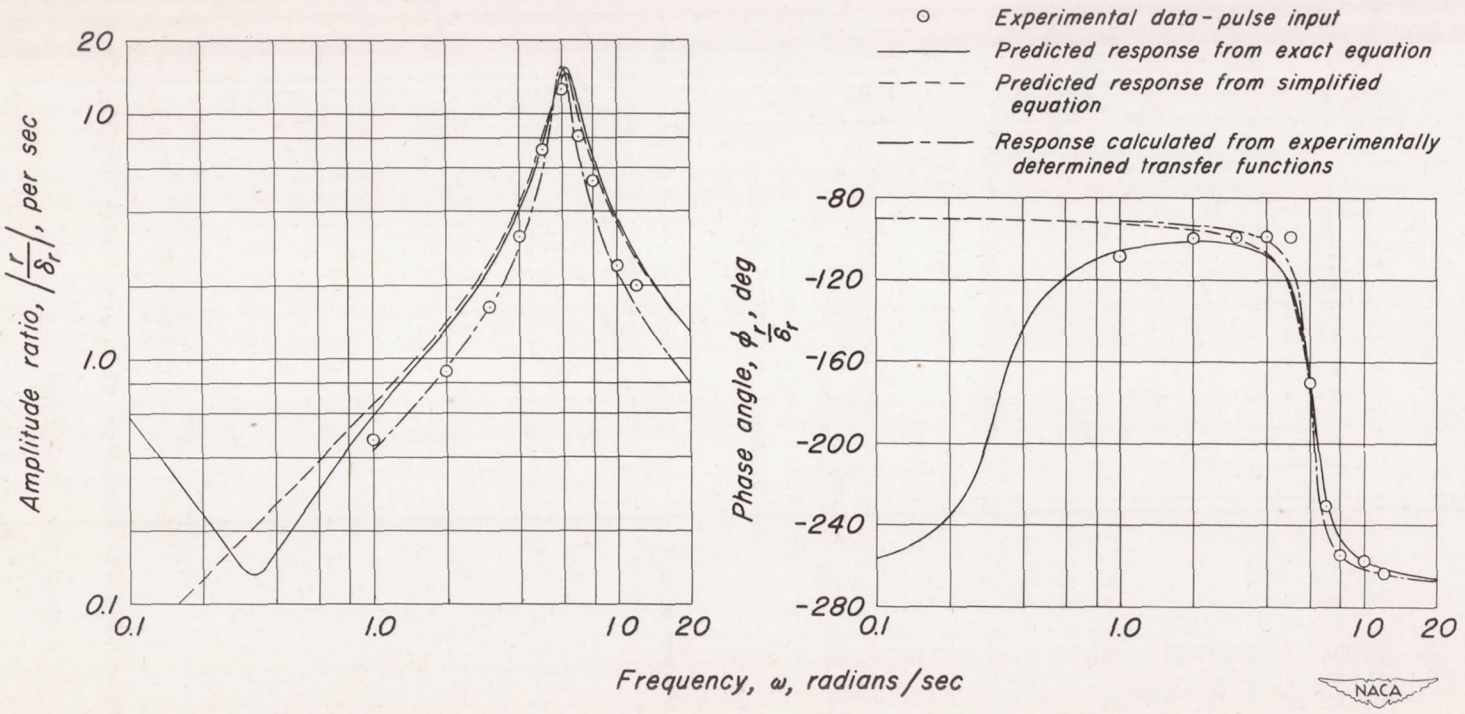
(e) Yawing velocity response to aileron input; altitude, 35,000 feet.

Figure 5.- Continued.



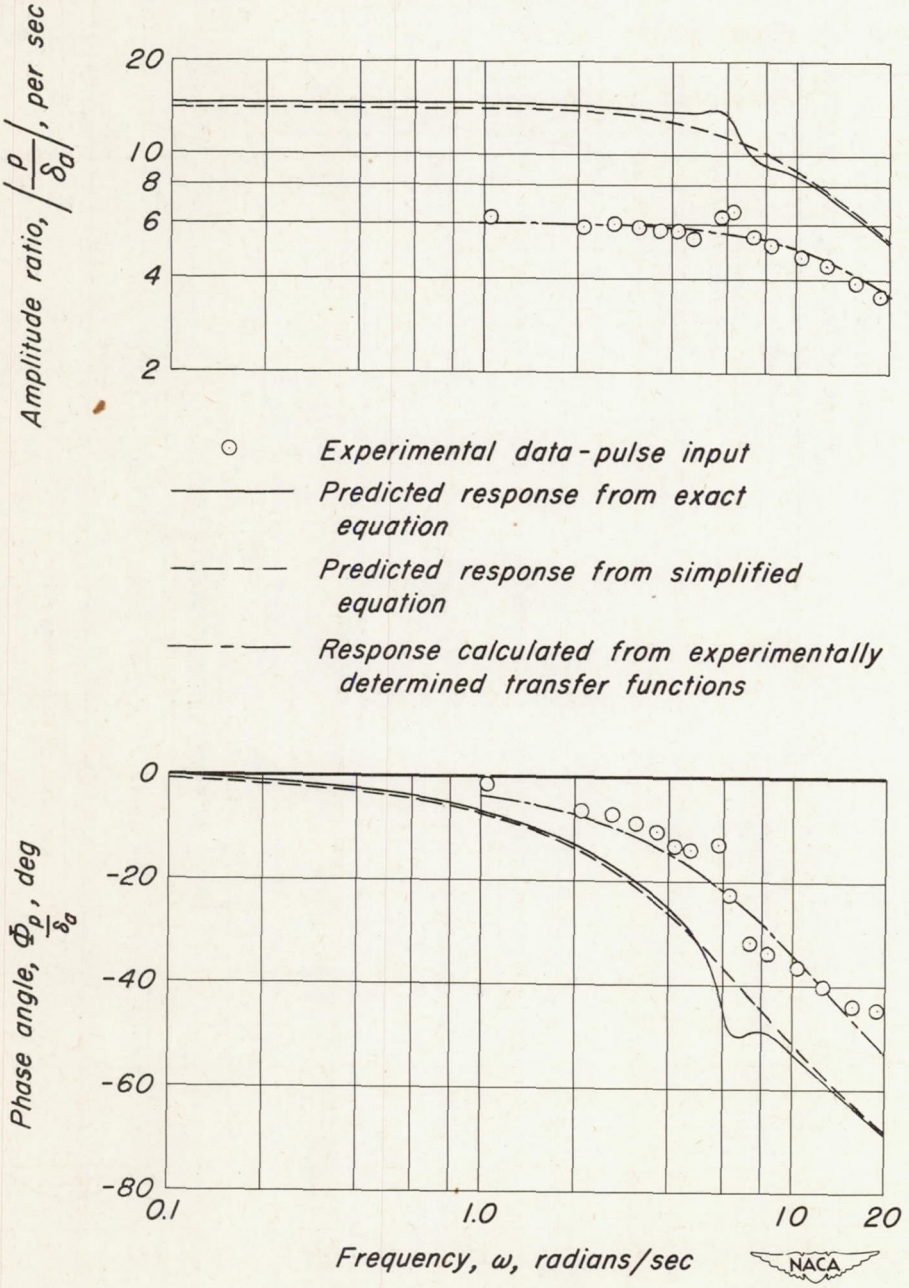
(f) Sideslip angle response to aileron input; altitude, 35,000 feet.

Figure 5.- Continued.



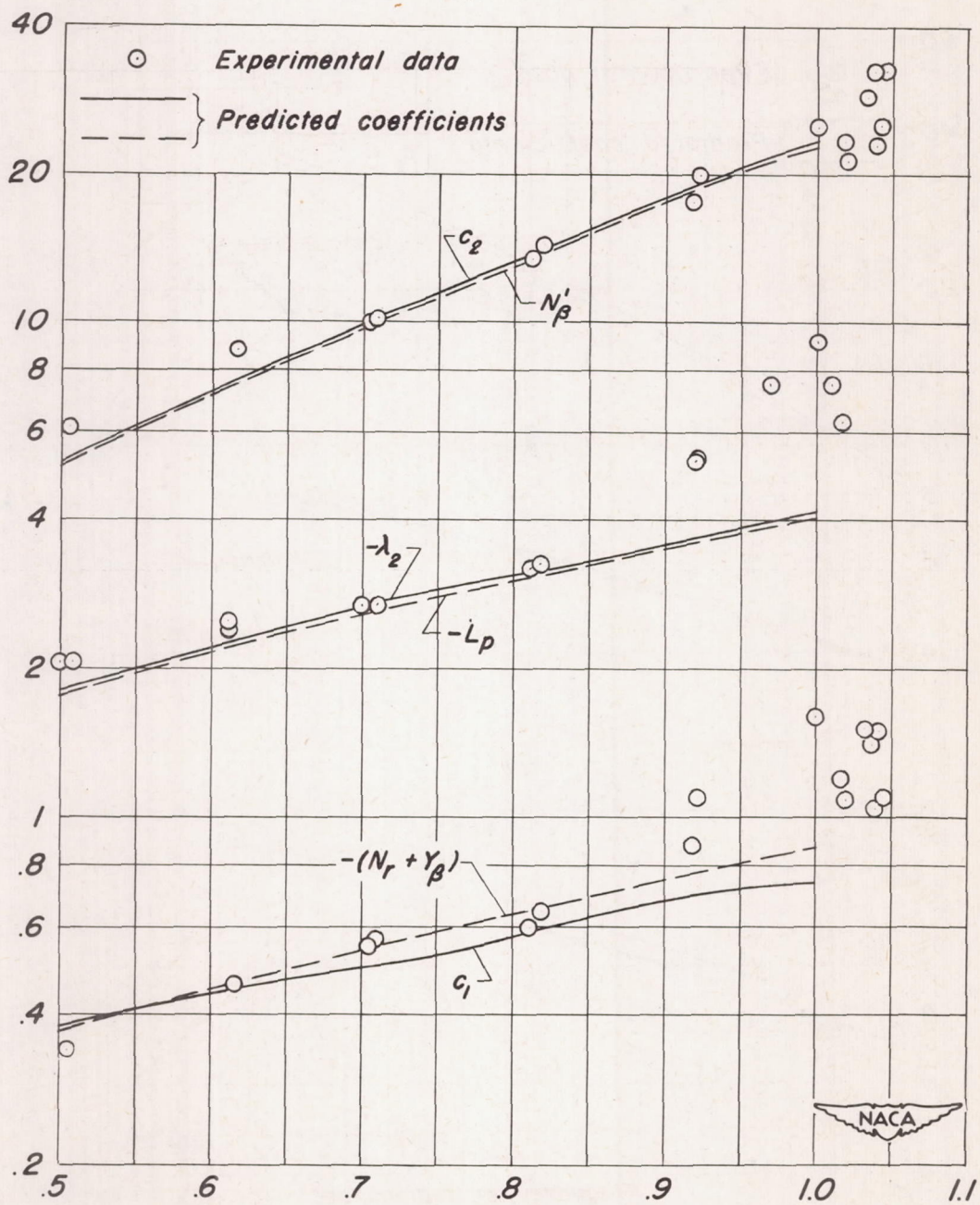
(g) Yawing velocity response to rudder input; altitude, 10,000 feet.

Figure 5.- Continued.



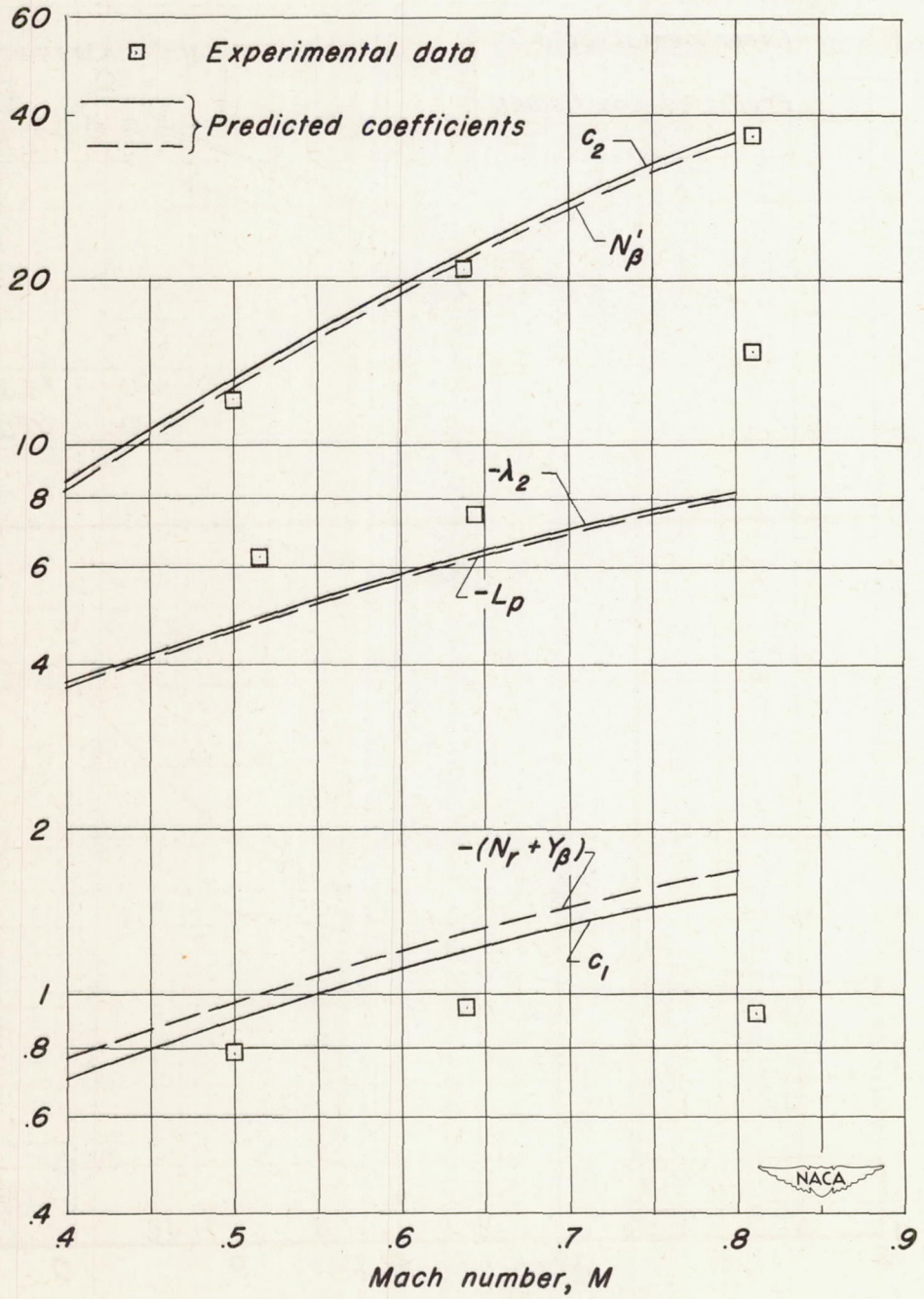
(h) Rolling velocity response to aileron input; altitude, 10,000 feet.

Figure 5.- Concluded.



(a) Altitude, 35,000 feet.

Figure 6.- Variation with Mach number of the coefficients of the characteristic equation λ_2, C_1, and C_2.



(b) Altitude, 10,000 feet.

Figure 6.- Concluded.

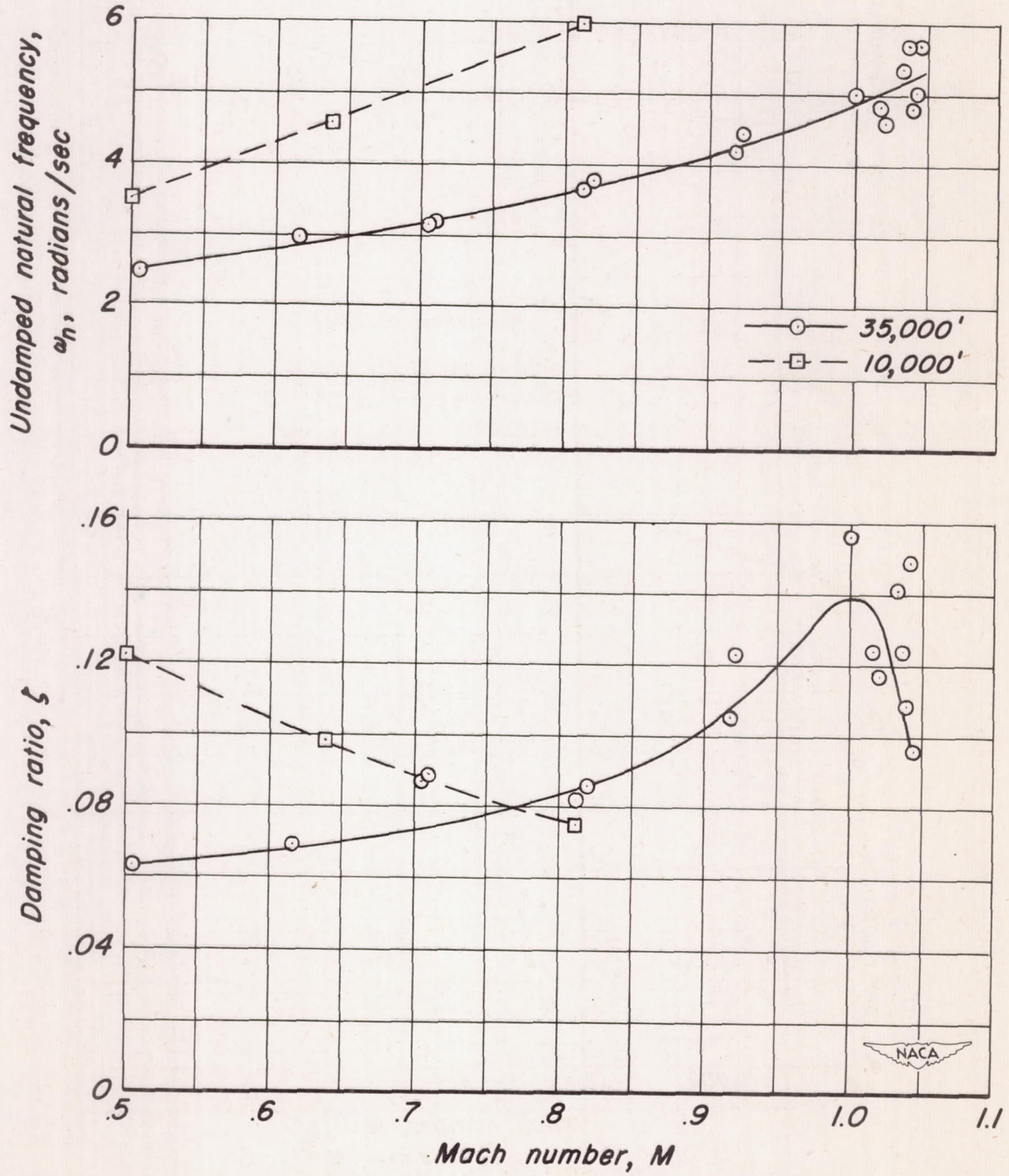


Figure 7.- Variation of undamped natural frequency and damping ratio with Mach number.

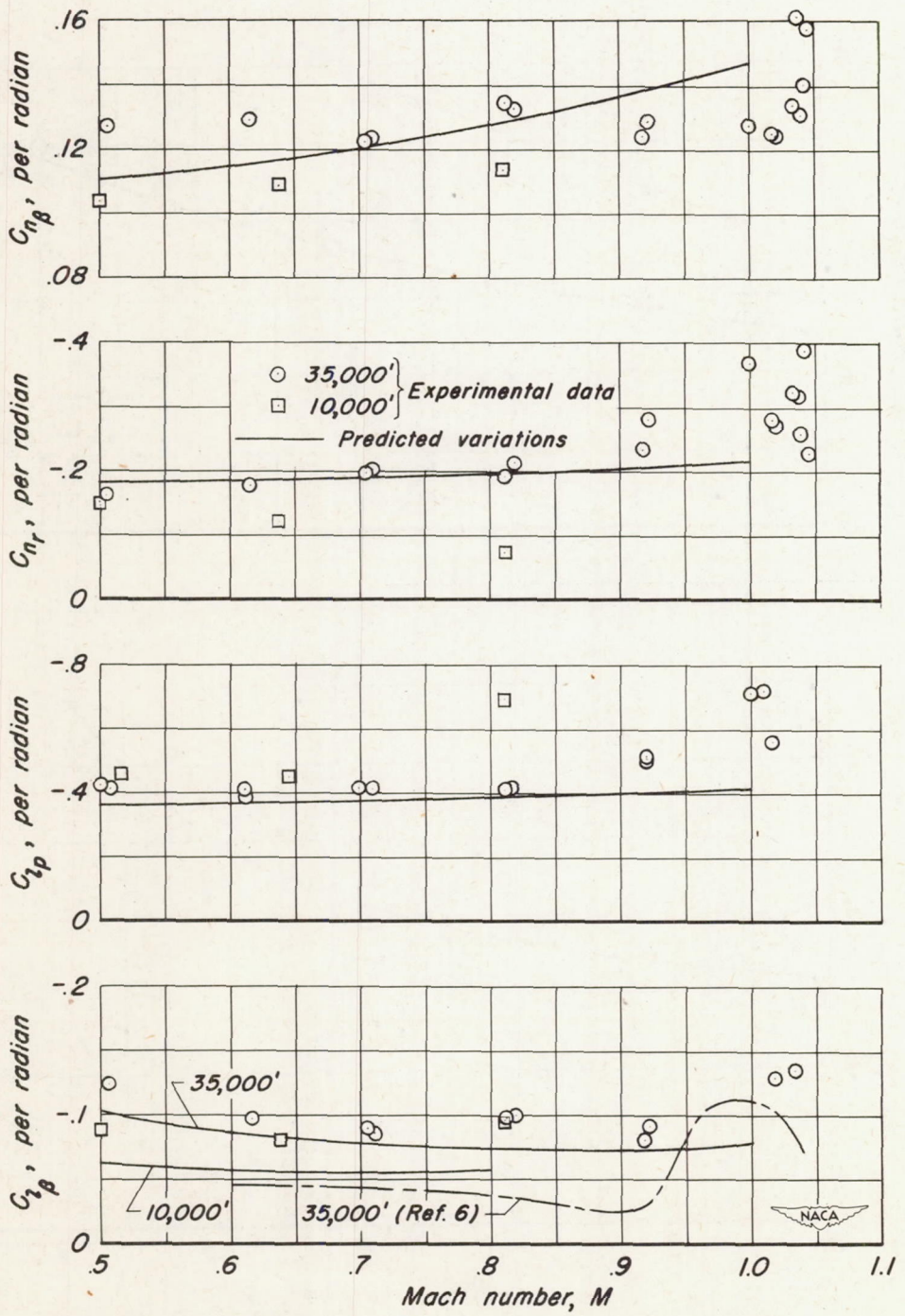


Figure 8.- Variation of the derivatives C_{n_β}, C_{n_r}, C_{l_p}, and C_{l_β} with Mach number.

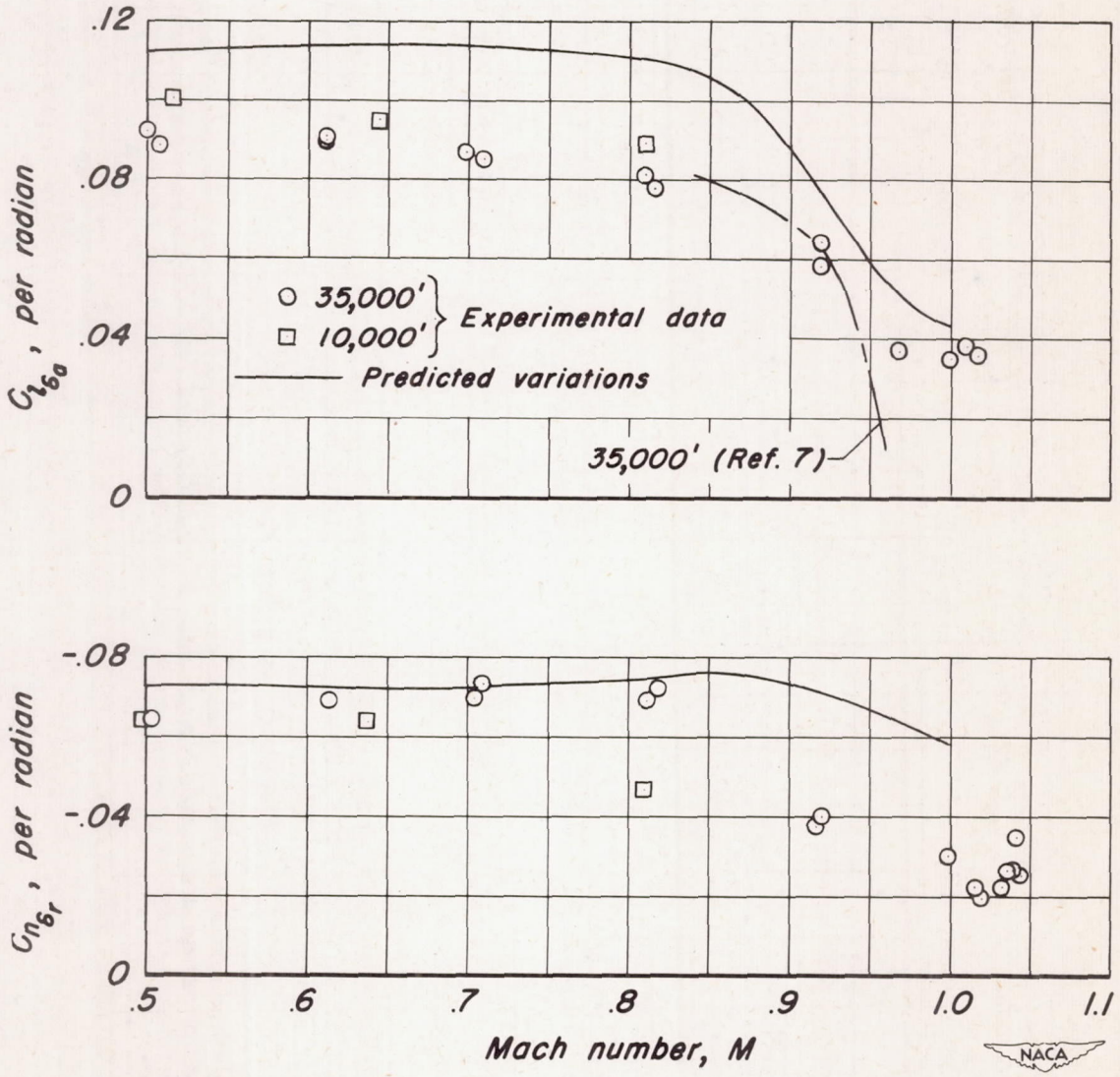


Figure 9.- Variation of the derivatives $C_{l_{\delta_a}}$ and $C_{n_{\delta_r}}$ with Mach number.

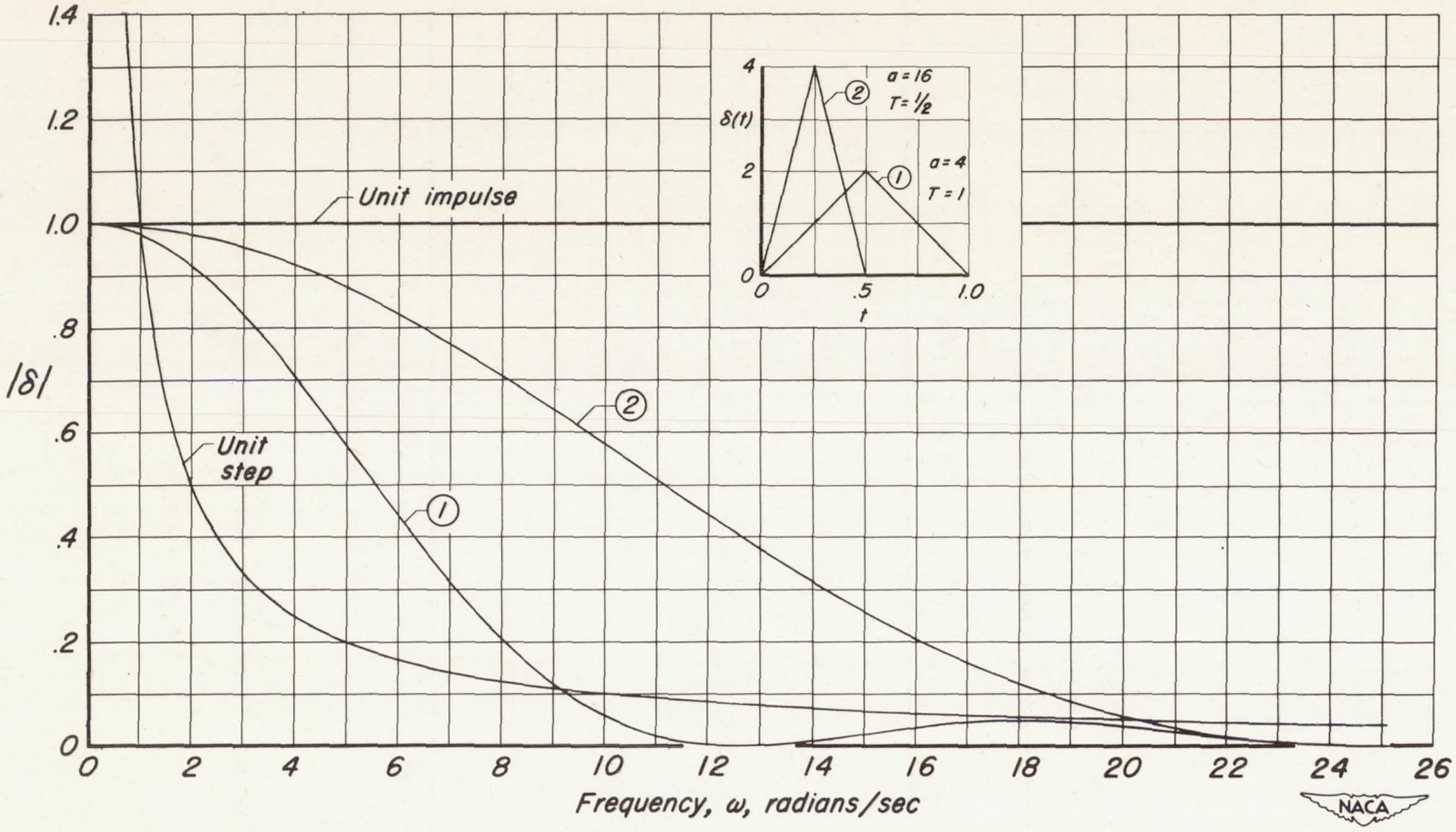


Figure 10.– Fourier transformation magnitudes of a step, an impulse, and two triangular shaped inputs.

NACA-Langley - 12-12-52 - 350

SECURITY INFORMATION

CONFIDENTIAL

UNCLASSIFIED

UNCLASSIFIED

This document contains information affecting the National Defense of the United States, within the meaning of the Espionage Laws, Title 18, U.S.C., Sections 793 and 794. Its transmission or the revelation of its contents in any manner to an unauthorized person is prohibited by law.

CONFIDENTIAL